

ND-A165 973

DEFLOCCULANTS FOR TAPE CASTING BARIUM TITANATE
DIELECTRICS(U) RUTGERS - THE STATE UNIV NEW BRUNSWICK NJ
J DEPT OF CERAMICS M R CANNON JUL 85 TR-4

1/1

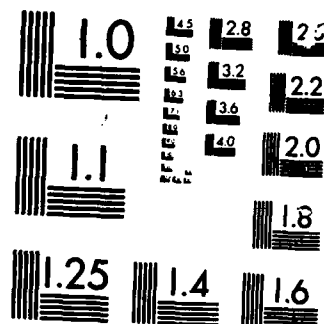
UNCLASSIFIED

N00014-82-K-0313

F/G 7/1

NL

END
2410
K. G.



MICROCOPY RESOLUTION TEST CHART

REPORT DOCUMENT

 READ INSTRUCTIONS
 BEFORE COMPLETING FORM
 RECIPIENT'S CATALOG NUMBER

12

AD-A165 973

1. REPORT NUMBER

4

4. TITLE (and Subtitle)

 Deflocculants for Tape Casting
 Barium Titanate Dielectrics

TYPE OF REPORT & PERIOD COVERED

 Annual Report *✓*
 March 1984-March 1985

6. PERFORMING ORG. REPORT NUMBER

171

7. AUTHOR(s)

W. Roger Cannon

8. CONTRACT OR GRANT NUMBER(s)

N0014-82-k-0313

9. PERFORMING ORGANIZATION NAME AND ADDRESS

 Department of Ceramics
 Rutgers, The State University of New Jersey

10. PROGRAM ELEMENT, PROJECT, TASK AREA & WORK UNIT NUMBERS

NR651-008

11. CONTROLLING OFFICE NAME AND ADDRESS

 Office of Naval Research
 800 North Quincy Street
 Arlington, Virginia 22217

12. REPORT DATE

July 1985

13. NUMBER OF PAGES

51

14. MONITORING AGENCY NAME & ADDRESS (if different from Controlling Office)

15. SECURITY CLASS. (of this report)

15a. DECLASSIFICATION/DOWNGRADING SCHEDULE

16. DISTRIBUTION STATEMENT (of this Report)

Unlimited

 This document is approved
 for public release and sale; its
 distribution is unlimited.

 DTIC
 ELECTE

MAR 31 1986

17. DISTRIBUTION STATEMENT (of the abstract entered in Block 20, if different from report)

Unlimited

18. SUPPLEMENTARY NOTES

19. KEY WORDS (Continue on reverse side if necessary and identify by block number)

 Dielectrics, Barium Titanate, Deflocculants,
 Dispersants, Tape Casting

20. ABSTRACT (Continue on reverse side if necessary and identify by block number)

The tape casting slip composition barium titanate powder, MEK-Ethanol solvent, phosphate ester dispersant, acrylic binder, PEG and butyl-benzyl-phthalate plasticizers and cyclohexanone was studied.

The nature of the dispersion mechanism for the phosphate ester was found to be largely electrostatic.

The order of addition of components affected viscosity, green strength of tapes, densities, sinter tape strength and dielectric constant.

DD FORM 1 JAN 73 1473

DTIC FILE COPY

SECURITY CLASSIFICATION OF THIS PAGE (When Data Enter)

Technical Report No. 4

Contract N00014-82-k-0313

DEFLOCCULANTS FOR TAPE CASTING

BARIUM TITANATE

W. R. Cannon
Department of Ceramics
Rutgers, The State University of New Jersey
P. O. Box 909
Piscataway, New Jersey 08854

July 1985

Annual Report for Period March 1984-1985

Prepared for the
Office of Naval Research
800 North Quincy Street
Arlington, Virginia 22217

Reproduction in whole or in part is permitted for any
purpose by the United States Government.

TABLE OF CONTENTS

	<u>Page</u>
Acknowledgment-----	1
Presentations (This Year)-----	1
Publications-----	1
I. Introduction-----	2
I.1 Achievements and Future Plans-----	2
First Year-----	2
Second Year-----	2
Third Year-----	3
I.2 Future Plans-----	4
II. Experimental Progress-----	5
II.1 Dispersion of Barium Titanate in the Solvent with No Other Additives (Kurt R. Mikeska)-----	5
II.1.1 Experimental Procedure-----	6
II.1.1.1 Starting Materials-----	6
II.1.1.2 Techniques for Measuring the State of Dispersion-----	8
II.1.1.2.1 Rheology-----	8
II.1.1.2.2 Equilibrium Sedimentation Volumes-----	10
II.1.1.3 Effect of Solvent Composition on Dispersion-----	10
II.1.1.4 Adsorption Isotherms-----	10
II.1.1.5 Electrical Conductivity-----	11
II.1.1.6 Electrokinetic Phenomena-----	11
II.1.2 Results and Discussion-----	13
II.1.2.1 Screening Tests-----	13
II.1.2.2 Assessment of Dispersability of Phosphate Ester-----	13
II.1.2.2.1 Rheology-----	13
II.1.2.3 Dependence of Dispersion on the MEK/Ethanol Ratio-----	17
II.1.2.4 Adsorption Model-----	19
II.1.2.5 Adsorption Isotherms-----	21
II.1.2.6 Adsorption as a Function of Solvent Concentration-----	22

TABLE OF CONTENTS--Continued

	<u>Page</u>
II.1.2.7 Electrophoretic Mobility-----	23
II.1.2.7.1 Conductivity and Mobility as a Function of Phosphate Ester Concentration-----	23
II.1.2.7.2 Conductivity and Mobility as a Function of Solvent Composition-----	26
II.1.3 Conclusions-----	28
II.2 Interaction of Dispersant with the Binder and Other Organic Additives in the Slip (John R. Morris, Jr.)-----	29
II.2.1 Introduction-----	29
II.2.2 Experimental Procedures-----	29
II.2.2.1 Batch Preparation-----	29
II.2.2.2 Property Measurement-----	31
II.2.3 Results and Discussion-----	34
II.2.3.1 Viscosity Measurements-----	34
II.2.3.2 Relative Viscosity-----	37
II.2.3.3 Green and Fired Density-----	40
II.2.3.4 Green Tensile Strength-----	41
II.2.3.5 Sintering-----	44
II.2.3.6 Sinter Tape Strength-----	47
II.2.3.7 Electrical Properties-----	48
II.2.4 Conclusions-----	49
References-----	50

Accession For	
NTIS	CRA&I <input checked="" type="checkbox"/>
DTIC	TAB <input type="checkbox"/>
Unannounced <input type="checkbox"/>	
Justification	
By	
Distribution /	
Availability Codes	
Dist	Avail and/or Special
A-1	

LIST OF TABLES

<u>Table</u>	<u>Page</u>
I. Lot Analyses for HBP (Lot 567) Barium Titanate Powder-----	6
II. Water Contents as Determined by Karl Fisher Methods-----	8
III. The Relative Viscosity for Slips with Three Different Addition Sequences-----	38
IV. The Dielectric Constant of Tapes Made with the Three Addition Sequences-----	48

LIST OF FIGURES

<u>Figure</u>	<u>Page</u>
1. Apparent Viscosity as a Function of Phosphate Ester Concentration for Dry, Aged, and Ambient Dispersions at 50.0 Vol. % Solids-----	14
2. Apparent Viscosity as a Function of Phosphate Ester Concentration at 50.0 Vol. % Solids-----	15
3. Apparent Viscosity as a Function of Phosphate Ester Concentration for Semi-Dry and Hydrated Suspensions at 25.0 Vol. % Solids-----	16
4. Equilibrium Gravity Settled Suspensions as a Function of Phosphate Ester Concentration-----	16
5. Apparent Viscosity as a Function of Solvent Fraction--	17
6. Apparent Viscosity as a Function of Phosphate Ester Concentration at 0.8% MEK-----	18
7. Apparent Viscosity as a Function of Phosphate Ester Concentration at 0.2% MEK-----	18
8. Phosphoric Acid and Its Corresponding Esters-----	19
9. Ionization of Phosphate Esters-----	20
10. A Schematic for the Adsorption of the Phosphate Ester onto Barium Titanate in the MEK-Ethanol Azeotrope-----	20
11. A Comparison Between Adsorption and Viscosity as a Function of Phosphate Ester Concentration-----	21
12. Adsorption as a Function of Solvent Fraction-----	22
13. Conductivity as Function of Phosphate Ester Concentration-----	25
14. Zeta Potential as a Function of Phosphate Ester Concentration-----	25
15. A Comparison Between Zeta Potential, Viscosity and Adsorption as a Function of Phosphate Ester Concentration-----	26

LIST OF FIGURES--Continued

<u>Figure</u>		<u>Page</u>
16.	Conductivity as a Function of Solvent Fraction-----	27
17.	Zeta Potential as a Function of Solvent Fraction-----	27
18.	The Processing and Addition Sequence Used in Preparation of Samples-----	30
19.	Method of Extrapolation Form Low Shear Rates to High Shear Rates-----	31
20.	Heating Schedule for Sintering of Tapes-----	32
21.	Schematic of Fixture Used for Biaxial Flexure Tests----	33
22.	The Scale for Rating Flatness-----	34
23.	Viscosity Measured at 384 Sec^{-1} as a Function of Aging Time of the Slip-----	35
24.	Viscosity Measured at 9.8 Sec^{-1} as a Function of Aging Time of the Slip-----	36
25.	The Relative Viscosity Measured for Sequence 1-----	38
26.	The Relative Viscosity Measured for Sequence 2-----	39
27.	The Relative Viscosity Measured for Sequence 3-----	39
28.	Density of Green and Sintered Tapes-----	40
29.	The Ultimate Tensile Strength of Green Tapes-----	41
30.	SEM Micrograph of the As-Cast Surface of the Various Tapes for Slips Aged 1 Day-----	42
31.	SEM Micrographs of the As-Cast Surface of the Various Tapes for Slips Aged 6 Days-----	43
32.	SEM Micrographs of the As-Cast Surface of the Various Tapes for Slips Aged 10 Days-----	43
33.	Micrograph of As-Sintered Surface-----	44
34.	Micrograph of As-Sintered Surface-----	45

LIST OF FIGURES--Continued

<u>Figure</u>	<u>Page</u>
35. Micrograph of As-Sintered Surface-----	45
36. Flatness as a Function of Addition Sequence and Slip Aging-----	46
37. The Biaxial Flexure Strength of Sintered Tapes as a Function of Addition Sequence and Aging Time-----	47
38. The Surface of a Sintered Tape Made from Slips Using the Simultaneous Addition Sequence-----	48

Acknowledgment

The major portion of the research described in this report was performed by Mr. Kurt Mikeska and Mr. John R. Morris, Jr. in partial fulfillment of the research requirement for a PhD. Mr. James Rydzak, a graduate student in Chemistry and Ceramics advised John R. Morris on the FTIR study. Undergraduate students who have contributed considerably to this report are Mr. David Eng and Ms. Angela Karas.

Presentations (This Year)

1. W. R. Cannon, "Dispersion and Rheology," presented at the Gordon Conference on Solid State Ceramics, July-Aug. 1985.
2. K. R. Mikeska, D. C. Eng, and W. R. Cannon, Dispersion Properties of BaTiO_3 , Presented at the Annual Meeting of the American Ceramic Society, Cincinnati, Ohio, May 1985.
3. J. R. Morris, Jr. and W. R. Cannon, "Affects of Component Addition Sequence on Green and Fired Properties of Barium Titanate Tapes," presented at the Annual Meeting of the American Ceramic Society, Cincinnati, Ohio, May, 1985.
4. J. R. Morris, Jr. and W. R. Cannon, "Powder-Binder-Dispersant Interaction in Nonaqueous Tape Casting Slurries of BaTiO_3 ," Presented at the Fall Electronics Meeting of the American Ceramic Society, San Francisco, CA, Oct, 1984.
5. J. B. Blum and W. R. Cannon, "Tape Casting of Barium Titanate", Present at the Materials Research Symposium, Boston, MA, Nov., 1984.

Publications

1. Kurt R. Mikeska and W. Roger Cannon, "Dispersants for Tape Casting Pure Barium Titanate", in Advances in Ceramics, Vol. 9, Forming of Ceramics, American Ceramic Society, 1984, pp. 164-183.
2. Susan Forti, John R. Morris and W. Roger Cannon, "The Green Strength of Cast Tapes" Bull. Amer. Ceram. Soc., 64 [5] 724 (1985).
3. Linda Braun, John R. Morris, and W. Roger Cannon, "Binder and Plasticizer Effects on the Viscosity of Tape Casting Slips" Bull. Amer. Ceram. Soc. 64 [5] 727-729 (1985).
4. J. B. Blum and W. R. Cannon, "Tape Casting of Barium Titanate," Electronic Packaging Materials, MRS Symposia Proceedings 40, Edit. E.A. Giess, K-N Tu, D. R. Uhlmann, Pittsburgh, PA. 1985.
5. Kurt R. Mikeska and W. Roger Cannon, "The Dispersion of BaTiO_3 with a Phosphate Ester", to be submitted to the J. Amer. Ceram. Soc.

I. Introduction

With the need for highly reliable dielectrics for multilayer capacitors, research is being conducted on improved dispersion of barium titanate powders in a tape cast slurry. In this study a non-aqueous tape casting slip system is being considered. The specific composition of the system was chosen to closely resemble commercial compositions as well as we know them. Since dispersion is the focus of the study, a search was undertaken during the first year to find an outstanding dispersant for the particular formulation we would use during the study. A phosphate ester* was chosen.

The first part of our study has been concerned with determining how the phosphate ester functions as a dispersant and why it is effective. In the second part of the study the interaction between the dispersant and other components in the tape casting system were studied. The other components used in our system were binder, plasticizers and a homogenizer. An important element of this study was to consider the importance of order of addition of components and how this effects the properties of the casting slip, the green tape and the sintered tape. Some of the properties which were measured were strength, density and dielectric constant.

1.1 Achievements and Future Plans

The goals of the first three years have generally been accomplished. A thorough study of role of the dispersant in a nonaqueous suspension of barium titanate powder has been largely accomplished to date which constituted the intended research for the first two years. In the third year interactions of the dispersant with other components in the slip was proposed. This phase of the research was expanded to a greater extent than expected by taking on an additional graduate student. The following was accomplished:

First Year

1. Approximately 70 commercial dispersants were screened and the three best, a phosphate ester, an ethoxylate, and Menhaden Fish Oil were chosen for further studies.
2. Viscosity measurements and settling volume measurements were performed as a function of phosphate ester concentration.
3. Based on viscosity measurements and electrophoresis measurements a model was proposed for the dispersion effectiveness of the phosphate ester.

Second Year

1. The effects of water in the solvent and of aging of the suspension on the viscosity was measured.
2. The shear thinning and thixotropic behavior of the slips near the minimum viscosity was determined.

*Emphos PS21-A, Whitco Chemical Co.

3. The rheological behavior of slips using fish oil as a dispersant was compared with the phosphate ester.
4. An adsorption isotherm for the phosphate ester was measured.
5. The model for phosphate ester was further developed including some estimates of the adsorption configuration and the free energy of adsorption.
6. Preliminary experiments showing the effects of order of addition of dispersant and binder were made.
7. The effects of aging conditions on the strength of the green tape was studied.

Third Year

1. The dispersion properties of barium titanate with the phosphate ester were studied as a function of the solvent composition across the MEK-ethanol binary.
 - a. The viscosity was determined as a function of phosphate ester for several MEK-ethanol mixtures across the binary.
 - b. The level of adsorption of phosphate ester on the surface of the powder was determined for several MEK-ethanol mixtures across the binary.
 - c. The zeta potential was determined by microelectrophoresis for several MEK-ethanol compositions across the binary.
 - d. Electrical conductivity of the phosphate ester solution was determined for several MEK-ethanol mixtures across the binary.
2. The zeta potential of barium titanate was determined as a function of phosphate ester concentration for the azeotrope solvent.
3. Further refinement of the mechanism of dispersion was possible from the above measurements, particularly with respect to the importance of electrostatic repulsion.

4. Order of addition of components in the slip was studied as it affects the viscosity of the slip, the ultimate tensile strength of the green tape, the biaxial fracture strength of the sintered tapes, the density of the green and sintered tapes, and the dielectric constant of the sintered tapes.

5. The relative viscosity of the slips were measured to determine the importance of the various components in dispersing the powder for several different order of addition sequences.

I.2 Future Plans

1. The mechanism by which the phosphate ester disperses the barium titanate powder has not been completely described. Attempts will be made to determine the thickness of the phosphate ester adsorbed layer on the surface of the powder in order to determine the contribution of steric stabilization. Combined potential energy versus distance between particles will be plotted using current DVLO and steric stabilization theory.

2. Mechanisms will be considered to describe why the electrophoretic mobility of the barium titanate peaks at a given phosphate ester concentration and at a given solvent concentration (see results section).

3. The effect of water on the rheological properties of the powder-solvent suspension has been observed but the role of the water in affecting the rheology has not been investigated. The adsorption concentration of water on the particle and the effect of water concentration in the suspension on rheology will be studied.

4. The effect order of addition of components on rheology of the slip and properties of the tape has been studied empirically but the reason have not been fully investigated. Adsorption and desorption of components on the surface of the powder will be studied as a function of aging time. Electrophoretic mobility will be determined as a function of aging time.

5. The role of steric stabilization by the binder and the plasticizers will be determined by measuring the theta temperature for various mixtures. It is hoped that this will help elucidate the mechanism change with various additions.

6. FTIR will be used to study the interaction between the components of the system: dispersant-binder, dispersant-powder, dispersant-plasticizers, etc.

This research will be carried out by two graduate students, Kurt R. Mikeska and John R. Morris, Jr. who are in their final phase of their Ph.D. studies. They will have the assistance of several undergraduate students: Angela Karas, Richard Hill and Robert MacNiven.

II. Experimental Progress

II.1 Dispersion of Barium Titanate in the Solvent with no other Additives. (Kurt R. Mikeska)

As indicated in the initial studies (1,2), the powders and liquids used in this study were chosen in an effort to duplicate materials used by commercial manufactures of tape cast multi-layer capacitors. Typical tape casting systems consist of a dielectric powder, dispersant, liquid media, binders, and plasticizers. Dispersion properties and adsorption phenomena may become increasingly complicated as the number of system components increases. To avoid possible complications, this part of the study was conducted on systems containing only pure powders, dispersants, and liquids. Binders, plasticizers, and other additives were eliminated in this section but were considered in section II.2.

Non-aqueous systems are typically stabilized by adsorbed polymers or macromolecules, and aqueous systems are stabilized by electrostatic forces. The application of electrical double layer mechanism to non-aqueous systems has drawn little attention until recently (3). Critics of the extension of electrical double layer theory to non-aqueous suspensions argue that low liquid dielectric constants lead to much weaker repulsive forces between charged particles. Low ionic concentrations create enormous Debye lengths. The application of a combination electrostatic and steric mechanisms has recently been suggested as a stabilization mechanism for aqueous systems (4,5). The application of the combined mechanism (electrosteric) to non-aqueous systems has drawn even less attention. However, it has been suggested that steric forces may be effective at small particle separation distances while electrostatic forces predominate at further separation distances.

This part of the study focuses on the fundamental dispersion properties of BaTiO_3 suspended in a solution of methyl ethyl ketone and ethanol, which has a moderate dielectric constant, and a phosphate ester as a dispersant. Although results are specific to this particular system they may be applicable to other non-aqueous dispersant systems.

II.1.1 Experimental Procedure

II.1.1.1 Starting Materials

HPB (high purity) barium titanate, lot 567 and lot 697, manufactured by Tam Ceramics Inc.* was used as the dielectric (adsorbate) throughout this study. Lot analysis as supplied by Tam Ceramics is indicated in Table 2.1. Included in this table for comparison are BET** specific surface areas and density*** measurements conducted during this study. This grade of barium titanate was manufactured by an oxalate co-precipitate process, calcined at 850°C, and subsequently spray dried.

X-ray diffraction patterns of the barium titanate powder indicated pure material and no impurities within the detection limits of the diffractometer.****

TABLE I
Lot Analyses for HPB (lot 567) Barium Titanate Powder

Loss on Ignition (TAM)	0.33%
+325 Mesh (TAM)	.01%
B.E.T. specific surface (TAM)	3.56 m ² /g
B.E.T. specific surface (this study)	3.5 m ² /g
Density (TAM)	5.5 g/cm ³
Density (this study)	5.9 g/cm ³
BaO/TiO ₂ mole ratio (TAM)	0.997
Fisher number (TAM)	1.19

* Tam Ceramics Inc., Niagra Falls, N.Y.

** Density measurements were conducted on a Micromeritics Instrument Corp. Autopycnometer 1320.

*** Specific surface area was measured on a Quantachrome Corp. Quantasorb Sorption System.

**** Diffraction measurements were conducted on a Philips Electronic Instruments diffractometer

The liquid used to disperse the barium titanate was an azeotrope mixture of methyl ethyl ketone and ethanol. The mixture of MEK and ethanol was chosen as the solvent because of its low inherent viscosity and low heat of vaporization. The azeotrope consisting of 66 wt% MEK and 34 wt% ethanol was chosen in order to avoid change in composition during evaporation of the solvent.

Fisher Reagent grade MEK was used throughout this study. MEK has a molecular weight of 72.11, a density of $.7996\text{g/cm}^3$ at 25°C , a viscosity of 0.20 cps at 25°C , a dielectric constant of 18.5 at 25°C . The chemical formula is $\text{CH}_3\text{CH}_2\text{COCH}_3$.

Fisher Reagent grade ethanol and Florida Distillaries absolute ethanol was used in this study. Ethanol has a molecular weight of 46.07, a density of 24.3. at 25°C , and a structural formula $\text{C}_2\text{H}_5\text{OH}$.

A phosphate ester, lot 04141 and lot C0284, manufactured by Whitco Chemical Co. was found to be an effective dispersant. The phosphate ester is an anionic surfactant when ionized. Phosphate esters are the esters of their corresponding oxy-acids. *Emphos PS-21A is the corresponding ester of phosphoric acid (6). Phosphoric acid is tribasic in which one, two, or three of the acidic hydrogens of the hydroxyl groups are replaced by alkoxy groups. Emphos PS-21A is an equal combination of both mono- and diethoxyl phosphate esters with a molecular weight of 525 to 530 for the mono- ethoxyl ester and 950 for the diethoxyl ester (6). The alkoxy function groups are thought to be a combination of ethoxylate groups and linear carbon chains, though the exact structure is not yet known. The phosphate ester has a density of 0.925g/cm^3 .

The initial report discussed effects of water on dispersion for ambient and dry materials. This study continues to investigate the effects of water. In this case known amounts of distilled-deionized water were added to suspension. Table 2.2 lists water content as determined by Karl Fisher Methods. The Karl Fisher procedure was discussed in the previous report (1).

*Emphos PS-21A, Whitco Chemical Co.

Table II

Water Contents as Determined by Karl Fisher Methods

	Ambient (%)	(Dry) %
Methyl Ethyl Ketone (Fisher Reagent Grade)	0.0338	0.0068
Ethanol (Fisher Reagent Grade)	5.1029	
Absolute Ethanol (Florida Distillaries)	0.20885	0.0161*
MEK-ethanol (azeotrope)	1.8658	0.0059*
MEK-absolute ethanol (azeotrope)	3.79 (Added water)	
Barium Titanate Powder	0.1229	0.1120**

II.1.1.2 Techniques for Measuring the State of DispersionII.1.1.2.1 Rheology

Viscosity as a function of phosphate ester concentration was used to determine the optimum point of dispersion under a variety of experimental conditions. A 2x HAT Brookfield cone-plate micro viscometer and a Haake coaxial cylinder rotational viscometer** were used to measure suspension rheology. In some instances both the Haake and the Brookfield were used to

* Solvent was dried over Linde molecular sieve.

** Powder was vacuum dried at 200°C for twenty-four hours.

* - Brookfield Engineering Laboratories, Inc.

** - HAAKE Mess-Technik GmbH H V. Co.

measure rheology under the same or similar experimental conditions. The results obtained from both instruments will be presented. In all instances the results indicate similar relative trends.

Before discussing individual experimental conditions, some general information and experimental parameters are presented for each type of viscometer.

BROOKFIELD CONE-PLATE - all rheology measurements made with the 2x HAT Brookfield cone-plate microviscometer utilized a CP-42 cone-plate arrangement. The Brookfield viscometer was used to measure viscosity as a function of phosphate ester concentration under dry, ambient, and aged conditions. Dispersion samples were analyzed at 50 Vol % solids and suspended in the MEK-ethanol azeotrope.

For each conditions, a series of dispersion samples of each concentration of phosphate ester were prepared, ranging from 0.2 vol % to 2.0 vol % phosphate ester. The dispersant was first added to the solvent and mixed by shaking. A known quantity of powder was then added to the solution of dispersant and solvent. The total sample volume was 16.36 ml. Samples were agitated ultrasonically with a probe for 2.0 minutes at 40 W/cm^2 and cooled in an ice bath during sonification. Each sample was subjected to the full range of its shear rates in order to determine slip rheology. Rheology measurements were taken immediately after agitation to avoid possible internal structure formation within the suspension which might occur with time.

HAAKE ROTOVISCOMETER - All rheology measurements made with the Haake rotoviscometer utilized a Haake Rotovisco RV/CV/LV 100 with a ZA 30 coaxial cylinder. The Rotovisco was interfaced with a Hewlett-Packard HP 86B computer.

In order to determine if the point of optimum dispersion varied with solids loading, viscosity as a function of dispersant concentration was measured at 25.0 vol. % solids and 50.0 vol. % solids using the Haake Rotovisco. The effect of water on dispersion properties was also evaluated at 25.0 vol. % solids and 50.0 vol. % solids by measuring viscosities of semi-dry and hydrated (added water) samples. For these experiments, the concentration of phosphate ester ranged from 0.15 vol. % to 2.0 vol. %. The total sample volume was 45.0 ml. The dispersant was added to the solvent and mixed by shaking. A known quantity of powder was subsequently added to the solution of solvent and dispersant. Samples were prepared in 50.0 ml polyethylene centrifuge tubes. To establish suspension equilibrium and reduce particle agglomeration, samples were ultrasonicated for one minute at 40 W/cm^2 , mixed in tumbling end over end fashion for 24 hours, and again ultrasonicated for one minute. Rheology measurements were taken immediately after agitation to avoid possible internal structure formation. A time versus shear rate profile was established to evaluate slip rheology. Shear rate was increased continuously from 0 to 300.0 sec^{-1} over a 2.0 minute interval, held at 30.0 sec^{-1} for 0.1 minutes, and subsequently decreased to 0 sec^{-1} over a 2.0 minute interval.

The effects of water on dispersion were initially studied using the Brookfield viscometer for samples prepared at 50.0 vol. % solids as discussed in

the previous report (9). The materials used in this experiment contained a considerable amount of water as shown in Table II. However, the ethanol used in this experiment was denatured. The denaturing process introduced other impurities into the alcohol (1.0 % ethyl acetate, 1.0 % methyl iso-butyl ketone, and 1.0 % aviation gasoline) may effect the state of dispersion in addition to the effects caused by the water. To eliminate the denaturing impurities and evaluate the effects caused solely by water, samples were prepared under "hydrated" and "semi-dry" conditions using the absolute ethanol-MEK azeotrope. The hydrated samples were prepared using absolute ethanol-MEK with known additions of distilled deionized water as indicated in Table II. In these experiments the absolute ethanol and MEK were used as received and not dried over molecular sieve as was the case in the earlier "dry" experiment measured with the Brookfield viscometer. Therefore, a distinction is made between the "dry" samples measured with the Brookfield viscometer and the "semi-dry" samples measured with the Haake viscometer. The barium titanate used in the hydrated and semi-dry experiments was vacuum dried for twenty four hours at 200°C.

II.1.1.2.2 Equilibrium Sedimentation Volumes

Gravity settled compacts were used to evaluate the dispersability of the phosphate ester suspensions. The samples were prepared and processed at 25.0 vol % solids in a manner identical to the samples in the semi-dry experiment discussed in Section II.1.1.2.1. All samples were allowed to settle under gravity for approximately three months in 200.0 ml. sealed pyrex culture tubes. Relative sediment height observations were subsequently recorded.

II.1.1.3 Effect of Solvent Composition on Dispersion

Viscosity of suspensions was measured as a function of composition of solvent across the MEK-ethanol binary to assess its effect on the capability of the phosphate ester to disperse the powder. Viscosity was measured with the Brookfield viscometer at several points along the binary solvent at 0.7 vol% (phosphate ester to powder) which had previously been found to be the optimum dispersant level. Samples were prepared at 50 vol. % solids in the semi-dry condition. In order to determine if the 0.7 vol. % phosphate ester concentration would be optimum at solvent compositions other than the azeotrope, viscosity as a function of phosphate ester concentration was measured at 20 % MEK - 80 % ethanol and 80 % MEK - 20 % ethanol. These samples were prepared and analyzed as discussed above.

II.1.1.4 Adsorption Isotherms

The surface excess concentration of the phosphate ester dispersant adsorbed onto a unit area of barium titanate was determined by measuring the change in phosphate ester concentration that occurs on adsorption when a known weight of the powder, phosphate ester and liquid were allowed to come to equilibrium at a constant temperature. An aliquot of the resulting supernatant was then analyzed for residual solute. The supernatant was analyzed for phosphorus with a precision of 5 g/ml of solution.

Since the number of molecules of phosphate ester are proportional to the number of atoms of phosphorus, grams of phosphorus can be converted to moles of phosphate ester whereby N_g is the number of grams of phosphorus per sample of solution and MW_p is the molecular weight of phosphorus.

$$\text{Moles}_{\text{Ester}} = \frac{N_g}{MW_p}$$

Isotherms were determined for the adsorption of the phosphate ester as a function of phosphate ester solution concentration and for the adsorption of the phosphate ester as a function of solvent composition across the MEK-ethanol binary. Samples in both experiments were prepared at 25.0 vol. % solids. Total sample volume was 45.0 ml. Samples for the adsorption of the phosphate ester as a function of phosphate ester solution concentration were prepared in a manner identical to semi-dry samples discussed in Section 2.3.1.

II.1.1.5 Electrical Conductivity

Electrical conduction of the solvent-dispersant system was measured to provide a relative indication of ionic concentrations in liquids. Conductance was measured as a function of phosphate ester suspension concentration and as a function of solvent composition. Samples were prepared and processed at 25.0 vol% solids in a manner identical to the adsorption isotherm samples discussed in Section 2.5. Aliquots of the resulting supernatants were extracted with a syringe and conductance was measured with a YSI 32 conductance meter* using a sample cell with a cell constant of 1.068 cm^{-1} at 25°C .

II.1.1.6 Electrokinetic Phenomena

In this study the microelectrophoresis measurements were made using a Rank Bros. Mark II Electrophoresis apparatus* equipped with a rotating prism. A closed flat rectangular cell fabricated of fused silica was used. The high cell resistivity of silica is preferable when using low conductivity (i.e. low dielectric constant) media. The cell geometry included a two electrode set-up. Electrodes were constructed of platinum and blacked with in a 0.2 % solution of chlorplatinic acid containing 0.02 % lead acetate.

The calculation of zeta potentials (7) from electrophoretic velocities in moderate dielectric constant liquids for non-conducting particles was derived by Henry (8) and takes the form:

$$\mu = \frac{\epsilon \zeta}{6 \pi \eta} f(\kappa, a)$$

* Luvak Inc., Boylston, MA. using Argon plasma emission spectroscopy.

where μ is the electrophoretic velocity, $\epsilon = \epsilon_r \epsilon_o$, η is the viscosity of the liquid, κ is the reciprocal thickness of the double layer, a is the particle radius.

For low and moderate dielectric constant is assumed to be small (thickness of the double layer large) and the Henry equation can be reduced to the Hukel equation. In unrationalized form the equation is

$$\mu = \frac{\epsilon \zeta}{6 \pi \eta}$$

In rationalized form the equation becomes

$$\mu = \frac{\epsilon \zeta}{1.5 \pi \eta}$$

The rationalized form of the Hukel equation was used to determine zeta potentials throughout this study. The calculations of zeta potentials from electrophoretic velocities were determined using the aforementioned equations after consideration of work done by Wiersema, Loeb, and Overbeek (9) and Obrien and White (10). Electrophoretic velocities were measured as a function of phosphate ester solution concentration and as a function of solvent composition across the MEK-ethanol binary. Samples were prepared and processed at 25.0 vol. % solids in a manner identical to the adsorption isotherm samples discussed in Section II.1.1.3 Aliquots of the resulting supernatants containing a very dilute suspension of barium titanate particles were extracted with a syringe and injected into the flat sample cell for analysis. Electrophoretic velocities were measured by presetting the rotating prism to a known speed and adjusting the electric potential until the particles were stationary. Cell parameters are included in Appendix 1, cell electrophoretic measurements were performed in a constant-temperature bath filled with ethanol at $25^\circ \pm 0.5^\circ\text{C}$.

- * Yellow Springs Chemical Co., Yellow Springs, Ohio
- * Rank Brothers, Cambridge, England.

II.1.2 Results and Discussion

II.1.2.1 Screening Tests

As described in a previous report (10) approximately 70 commercial dispersants were evaluated for compatibility with the MEK-ethanol azeotrope by a solubility screening test. Twenty-nine of those dispersants determined to be soluble were further tested by a rheological screening test. The three most effective dispersants, in order of their effective dispersability, were found to be a phosphate ester*, a fatty acid**, and an ethoxylate***.

II.1.2.2 Assessment of Dispersability of Phosphate Ester

II.1.2.2.1 Rheology

From the screening of the various commercial dispersants, it was determined that using the phosphate ester the viscosity decreased most rapidly with concentration (8,9,10).

Thus, the dispersion properties of the phosphate ester were further studied by rheological and settling methods. Preliminary viscosity measurements indicated the phosphate ester was sufficiently effective to allow rheological measurements to be made at a very high volume fraction of solids (50 vol. % solids). Viscosity measurements were also performed at 25.0 vol. % solids for comparison purposes. Many of the adsorption, electrophoretic, and settling experiments were conducted at 25.0 vol. % solids, therefore, it was of interest to evaluate the dispersability of the phosphate ester at 25.0 vol. % solids.

Figure 1 from reference 9 shows measured apparent viscosity as a function of phosphate ester concentration under ambient, dry, and aged conditions measured at 50.0 vol. % solids with the Brookfield viscometer. These results are compared with Figures 2 and 3 which contain results for both 25 and 50 vol% solids and both hydrated and semi-dry conditions (II.1.1.2.1)

* Emphos PS-21A, Whitco Chemical Co.

** Menhaden Fish Oil, Spencer Kellogg Co.

*** Zonyl A, E. I. du Pont de Nemours & Co.

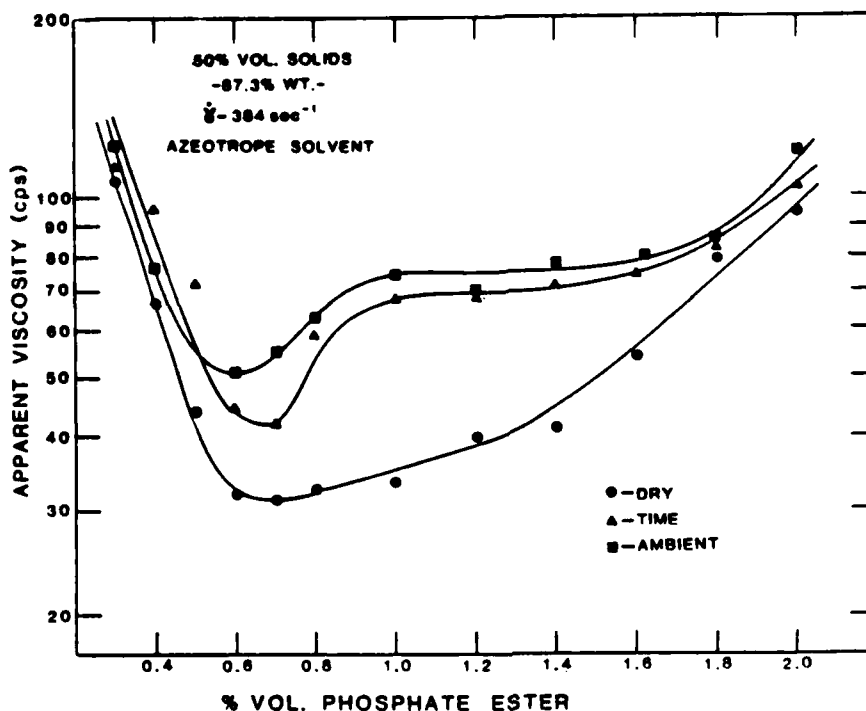


Figure 1 Apparent viscosity as a function of phosphate ester concentration for dry, aged, and ambient dispersions at 50.0 vol. % solids.

Figure 2 shows measured apparent viscosity as a function of phosphate ester concentration under semi-dry conditions at 50.0 vol. % solids measure with the Haake Rotovisco, and Figure 3 shows measured apparent viscosity as a function of phosphate ester concentration under semi-dry and hydrated (additions of known quantities of water) conditions at 25.0 vol. % solids using the Haake Rotovisco. Water content, as determined by Karl Fischer methods, is shown in Table II.

A comparison of Figures 2 and 3 indicate a optimum point of dispersion at approximately 0.75 vol. % phosphate ester for the semi-dry suspensions at 50.0 vol. % solids and 25.0 vol. % solids. These results conclude that the optimum point of dispersion is not effected by solids content at 50.0 and 25.0 vol. % solids.

Figure 3 also shows a definite increase in viscosity of the hydrated suspensions over the semi-dry suspension at 25.0 vol. % solids. According to these viscosity measurements, it can be concluded that the semi-dry dispersion are dispersed to a greater degree then the hydrated samples containing known additions of pure water. An attempt to make viscosity measurements on hydrated suspensions at 50.0 vol. % solids was also performed. However, the viscosity of the suspensions proved to be beyond the torque range of the Haake Rotovisco. Even through the actual measurements could not be made, indications were that the presence of water drastically increases viscosity (decreases the degree of dispersion) at 50.0 vol. % solids.

An apparent discontinuity occurs in Figure 3 for viscosity versus concentration curve for the suspension containing water. The curve indicates two optimum points of dispersion at approximately 0.15 vol. % and .75 vol. %, respectively. Gravity settled suspensions, as shown in Figure 4, indicate the discontinuity in the flocculation curve is real. Qualitatively, it can be concluded that the presence of water in the suspension causes this anomaly in the dispersion curve. Also, the "hump" seen in the flocculation curve of the ambient samples measured by the Brookfield viscometer and shown in Figure 1 can probably be attributed to the same phenomena. A more detailed discussion on the effects of water is contained in reference 1 but no explanation can be offered as yet for this behavior.

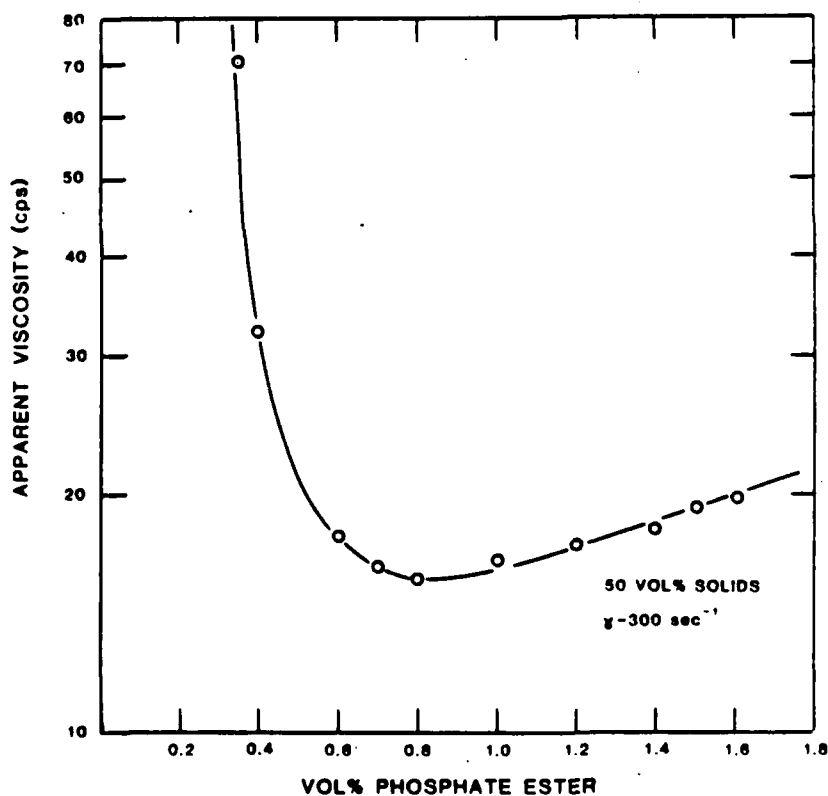


Figure 2 Apparent viscosity as a function of phosphate ester concentration at 50.0 vol. % solids.

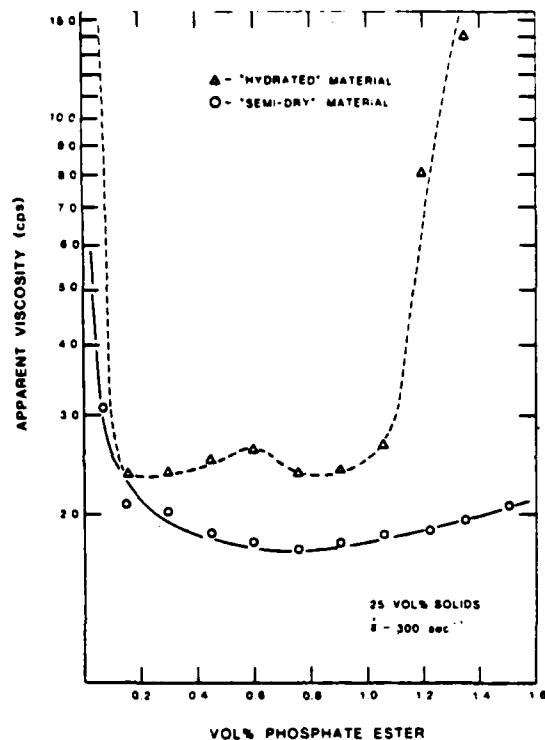


Figure 3 Apparent viscosity as a function of phosphate ester concentration for semi-dry and hydrated suspensions at 25.0 vol. % solids.

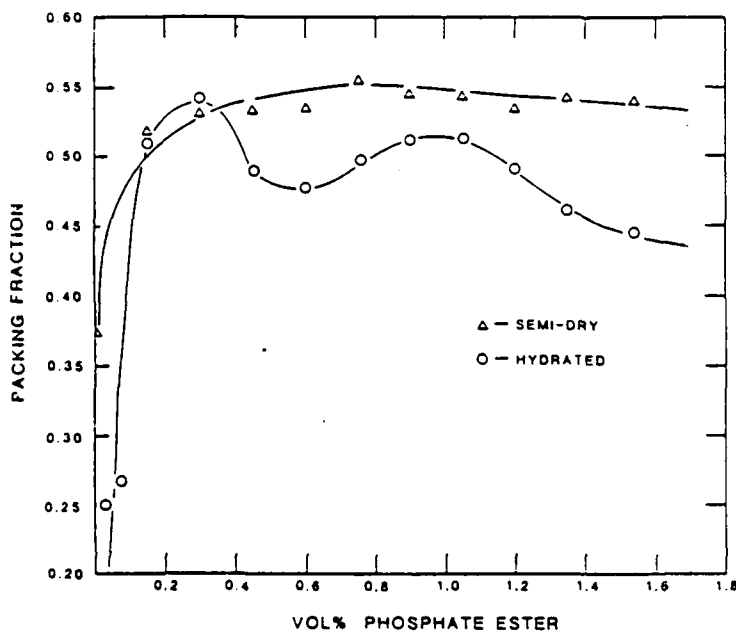


Figure 4 Equilibrium gravity settled suspensions as a function of phosphate ester concentration.

II.1.2.3 Dependence of Dispersion on the MEK/ethanol Ratio

The dispersion behavior of suspensions was studied as a function of the MEK/Ethanol solvent ratio. Viscosity was measured on barium titanate suspensions prepared at 50.0 vol. % solids at a constant 0.7 vol. % phosphate ester. Figure 5 shows viscosity versus volume fraction of ethanol in the MEK-ethanol solvent mixture. A minimum in viscosity, occurred at approximately the azeotrope solvent solution (66 % MEK, 34 % ethanol). The degree of dispersion decreases on either side of the azeotrope. The original choice of the azeotrope was based on a practical consideration, that the solvent not change composition as it vaporizes. These results however, conclude that the azeotrope is the optimum solvent mixture with respect to dispersion also.

To determine whether the above observation was merely related to the fact that we had only optimized the phosphate ester concentration using the azeotrope solvent and not other solvents, viscosity was measured as a function of phosphate ester concentration at solvent ratios other than the azeotrope. Viscosity as a function of phosphate ester for suspensions prepared at 50.0 vol. % solids and fraction ethanol of 0.8 and 0.2 are shown in Figures 6 and 7, respectively. These solvent ratios are on either side of the azeotrope solution. Both figures show minimum viscosities at approximately 0.7 vol. % phosphate ester similar to the azeotrope solvent. These results indicate the point of best dispersion as determined by viscosity measurements for all solvent ratios and phosphate ester concentration is the azeotrope solvent and a phosphate ester concentration of approximately 0.7 vol. %.

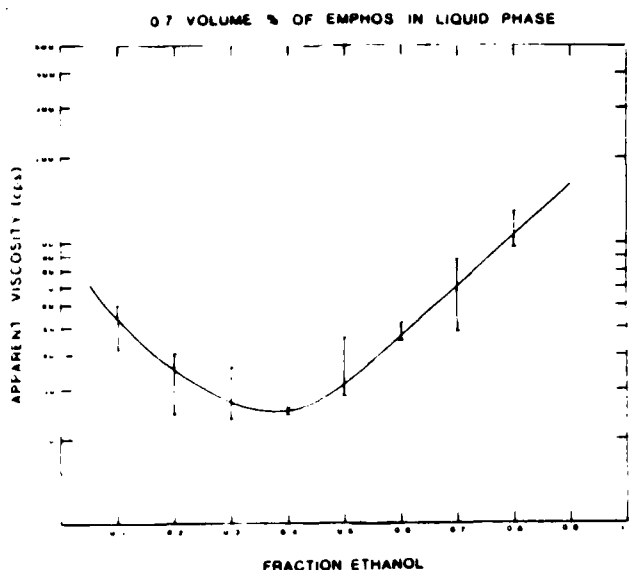


Figure 5 Apparent viscosity as a function of solvent fraction.

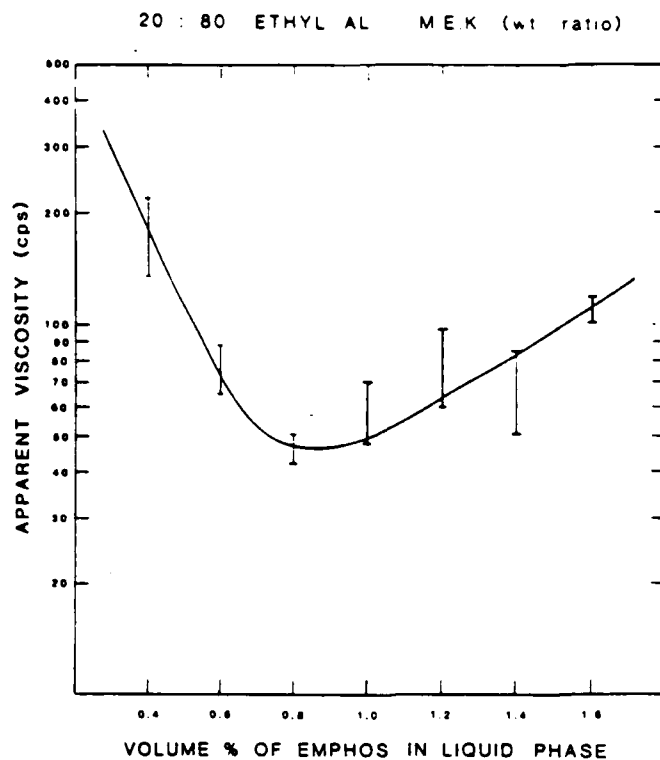


Figure 6 Apparent viscosity as a function of phosphate ester concentration at 0.8 % MEK.

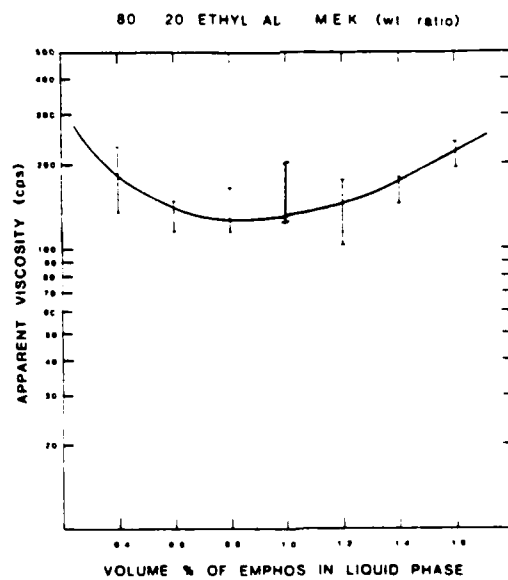
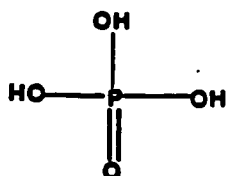


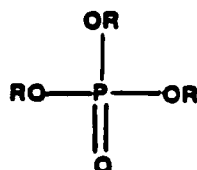
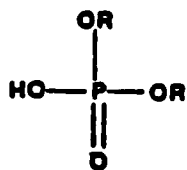
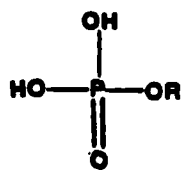
Figure 7 Apparent viscosity as a function of phosphate ester concentration at 0.2 % MEK.

II.1.2.4 Adsorption Model

To better understand the mechanism by which the phosphate ester stabilizes the barium titanate dispersion, a model for adsorption of the phosphate ester at the barium titanate/liquid interface was developed and presented in the previous report. The hydrogen of the hydroxyl groups of the mono- and diethoxyl esters shown in Figure 8 are highly acidic and readily dissociate in aqueous media resulting in the formation of anionic polymers, as shown in Figure 9. Confirmation of proton dissociation was indicated by a substantial drop in pH in both aqueous and non-aqueous (MEK-ethanol) medias on addition of the phosphate ester. The liberated proton is attracted to the metal oxide as indicated by acid-base reactions forming a positive surface charge. The lyophobic anionic portion of the long chain amphipathic polymer (phosphate ester), created on dissociation, is attracted by electrostatic forces (coulombic attraction forces) to the positive surface forming an electrostatic ionic type bond at the positively charged surface. The nonpolar lyophobic hydrocarbon tail is soluble in the relatively nonpolar MEK-ethanol solvent and extends readily from the surface of the solid into the organic media as shown in Figure 10.



PHOSPHORIC ACID



PHOSPHATE ESTERS

Figure 8 Phosphoric acid and its corresponding esters.

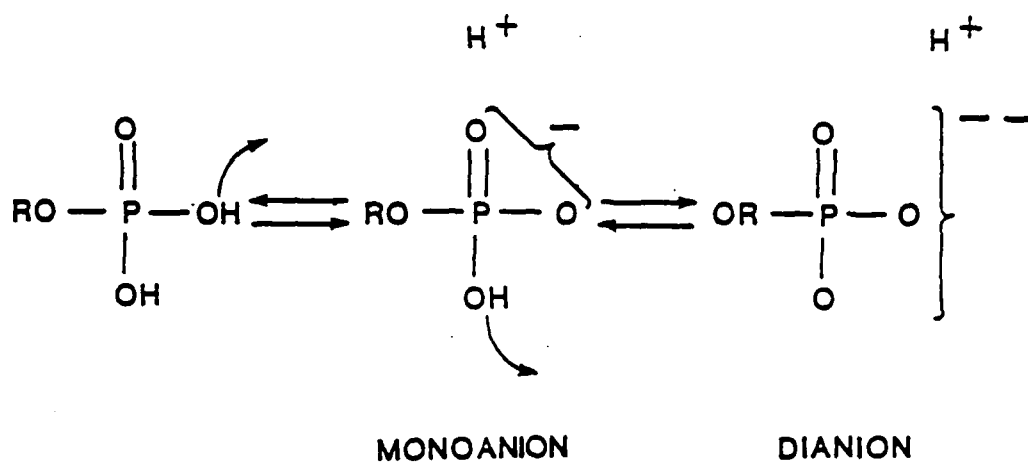


Figure 9 Ionization of phosphate esters.

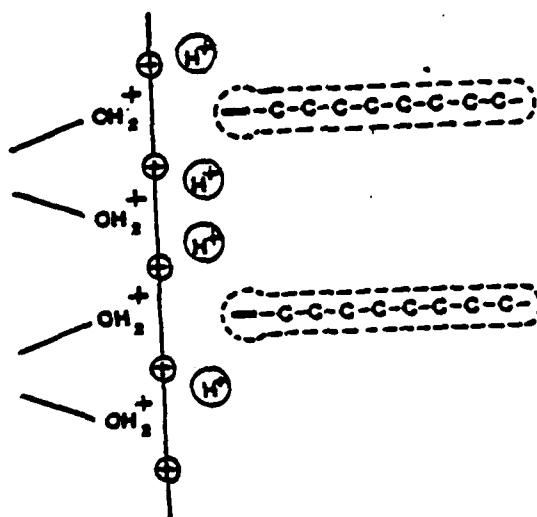


Figure 10 A schematic for the adsorption of the phosphate ester onto barium titanate in the MEK-ethanol azeotrope.

II.1.2.5 Adsorption Isotherms

The composite isotherm for the adsorption of the phosphate ester onto the barium titanate surface as a function of the equilibrium concentration of phosphate ester was discussed in detail in the previous report (1). In review, the isotherm indicated monolayer surface excess concentration of 1.09 moles/m^2 at an initial equilibrium concentration of approximately 3.5×10^{-4} mole fractions of phosphate ester. The adsorption plateau indicates there is no further adsorption of the phosphate ester beyond a monolayer of coverage. A monolayer of coverage corresponds to an adsorption area of 152 Å per phosphate ester molecule. These results were correlated with the more recent rheological results for 25 vol% solids and are shown in Figure 11. (In the previous report they were compared with the results for 50 vol% solids whereas the isotherm was generated for 25 vol%). The concentrations of phosphate ester at which monolayer coverage and minimum viscosity occurred is at the onset of monolayer coverage. It can be concluded for the phosphate ester-barium titanate system that a monolayer of coverage corresponds very well with optimum dispersion stability. From these results it can be postulated that the phosphate ester forms a steric barrier and thus provides good dispersion. As the level of adsorbed phosphate ester increases the viscosity decreases. With further addition of phosphate ester, the amount of phosphate ester adsorbed on the solid surface remains constant, as indicated by the long flat plateau, but the viscosity increases. The adsorption isotherm adequately explains the existence of a flocculation condition prior to the onset of monolayer coverage, however, it fails to provide information as to why flocculation increases at higher concentrations of phosphate ester occurring beyond the addition required for the initial monolayer of coverage.

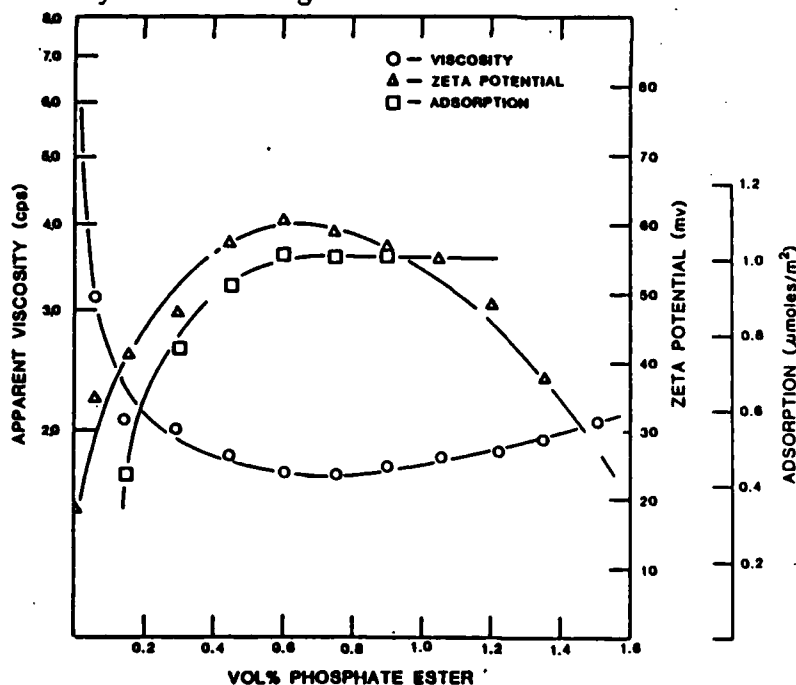


Figure 11 A comparison between adsorption and viscosity as a function of phosphate ester concentration.

It can be proposed that beyond the concentration of solute at which monolayer coverage occurs co-adsorption of solute, reorientation of adsorbed material (11), or the collapse of the possible electrical double layer may account for the increase in viscosity and agglomeration of particles. Electrical conduction and zeta potential measurements were subsequently conducted in an effort to test for a possible electrostatic mechanism. Results of these experiments are discussed in Section II.1.2.7.

II.1.2.6 Adsorption as a Function of Solvent Concentration

Viscosity measurements indicated a minimum viscosity was observed when the azeotrope solvent composition (0.66 MEK) of MEK-ethanol binary was used. At solvent fraction greater than and less than the azeotrope composition flocculation occurred. It was of interest to investigate the cause of flocculation at solvent fractions other than the azeotrope. For instance, the solubility of the phosphate ester in the solvent might effect the adsorption of the solute onto the solid. Solutes tend to adsorb onto powders better from poor solvents.

In Figure 12 adsorption as a function of solvent fraction is shown. The phosphate ester concentration is held constant at 0.7 vol. %, the concentration at which best dispersion was observed. Figure 12 indicates approximately a constant surface excess concentration of approximately 0.9 moles/m^2 . Though there is a slight increase in adsorption with increasing ethanol, the scatter of points shown in the curve is within the experimental error of 5 mg/ml, therefore a horizontal curve is assumed. The surface excess concentration, of approximately 0.9 moles/m^2 determined in this experiment is comparable to the corresponding surface excess concentration determined for 0.7 vol. % phosphate ester in the adsorption versus concentration of phosphate ester experiment. It can be concluded from these results that adsorption of the phosphate ester onto the barium titanate surface is not effected by MEK/ethanol solvent composition. Thus the increased viscosity observed on either side of the azeotrope solution cannot be attributed to changes in the amount of phosphate ester adsorbed. An

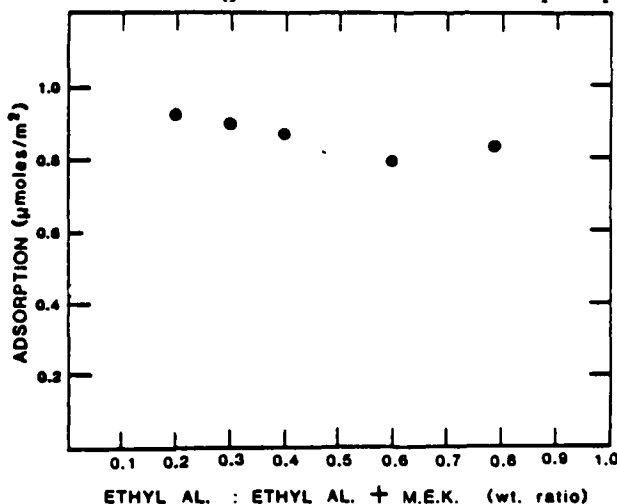


Figure 12 Adsorption as a function of solvent fraction.

alternate explanation is that a variation in the extension of the adsorbed polymer chain into the bulk solvent, or the collapse of a possible electrical double layer may account for the increase in flocculation on either side of the azeotrope solution.

Electrical conductivity and zeta potential measurements were subsequently conducted in an effort to test for a possible electrical double layer mechanism.

II.1.2.7 Electrophoretic Mobility

II.1.2.7.1 Conductivity and Mobility as a function of Phosphate Ester Concentration

The application of electrical double layer theory to particles dispersed in non-aqueous apolar (low dielectric constant, i.e. <15) solvents are less well understood than their aqueous counterparts. A review of the literature indicates the majority of investigations, both theoretical and practical, are devoted to aqueous systems. As a result, aqueous systems are well understood.

The MEK-ethanol azeotrope solution used in our system has a dielectric constant of approximately (20.5) estimated by linear extrapolation between the end members values (i.e. -24.3 at 25°C for ethanol and -18.5 at 25°C for MEK). In comparison, water has a ϵ of 78.5. This places our system closer to nonpolar solvents (i.e. hexane, benzene, etc.) than an aqueous system. The moderate dielectric constant of the MEK-ethanol azeotrope predicts our dispersion may have characteristics associated with polar solvent. A review of some difficulties in understanding non-aqueous dispersions is presented in the literature (11).

In non-polar solvent the particle are charged due to previously adsorbed ions or to adsorption of ions which exist in the non-polar solvent. According to the model presented earlier hydrogen ions dissociate from the phosphate ester and are adsorbed by the particle which increasingly charges the particle positively. The anionic phosphate ester is attracted and held tightly to the particle by ionic attraction. If enough phosphate ester is adsorbed on the surface the particle charge can be reversed. Recent FTIR studies indicate a stretching of the O-H bond which could be an indication of ionization. This evidence will be presented in the next progress report.

Initial electrophoresis measurements conducted on the MEK-ethanol, phosphate ester, barium titanate system, as discussed in the previous report indicated the existence of a positive surface charge on addition of the phosphate ester to the barium titanate, MEK-ethanol suspension. In order to test the extent of ionization of the phosphate ester in the solvent, conductivity was measured as a function of phosphate ester concentration and is shown in Figure 13. Results indicated an increase in conductance with an increase in phosphate ester concentration. The conductivity may be attributed to the dissociation of the acidic phosphate ester. Conductivity increases as the number of dissociated ions increases due to the increase in phosphate ester concentration. Thus, the ionic strength of the dispersion increases as the phosphate ester concentration increases. At very low concentrations of phosphate

ester, the data indicates relatively no conductivity. It can be postulated that at very low phosphate ester concentration, the dissociated ions are completely adsorbed by the powder and thus cannot contribute to the conductance of the bulk liquid.

An additional contribution to the electrical conductivity may arise from ions leached into the bulk liquid from the barium titanate surface. However, the dissociation of barium titanate surface groups is probably negligible compared to the phosphate ester contribution. In order to substantiate this hypothesis, dispersion supernatants will be analyzed for barium in future work.

In Figure 14 it is shown that zeta potential increases as phosphate ester concentrations increases from zero to approximately 0.7 vol. %. At this point a maximum in the of approximately 60 MV was observed, followed by a decrease in potential with further increases in phosphate ester concentration.

The presence of a charged surface in an ionic solution, as shown by the zeta potential and conductivity data, indicates the existence of an electrical double layer. An estimate of the extent of the diffuse layer from conductivity measurements ¹². These measurements assume that the rate controlling specie for conductivity is the counter ion. If in our system the counter ion is the phosphate ester and it is the rate controlling specie then the double layer thickness can be estimated from the following equations:

$$\frac{1}{\kappa} = \sqrt{\frac{\epsilon D}{2 \sigma}}$$

Where $1D$ is the diffusion constant for the charge carrying species and κ is the conductivity. The D value can be estimated from the Stoke-Einstein equation for spheres

$$D_0 = kT/6\pi\eta r$$

corrected with an appropriate value of f/f_0 for rods:

$$D = D_0 \times f/f_0$$

For the phosphate ester if we assume a length of 20 A, a single charge per molecule and $f/f_0 = 1.2$, then the double layer thickness, 40 , at a phosphate ester concentration of 0.7 vol% is 13 A. This double layer thickness is comparable to those commonly observed in aqueous systems.

Figure 14 compares the zeta potential data with the viscosity and adsorption data. A definite correlation can be drawn between the them. As discussed above the optimum dispersion coincides with monolayer coverage and it is now shown that it corresponds with the maximum in the zeta potential. The increase in viscosity at high phosphate ester concentration might now be explained by double layer theory in that the increased ionic concentration

shrinks the double layer and causes increased flocculation. The behavior is commonly observed in aqueous systems. Never the less, steric stabilization may also play a role in reducing the viscosity.

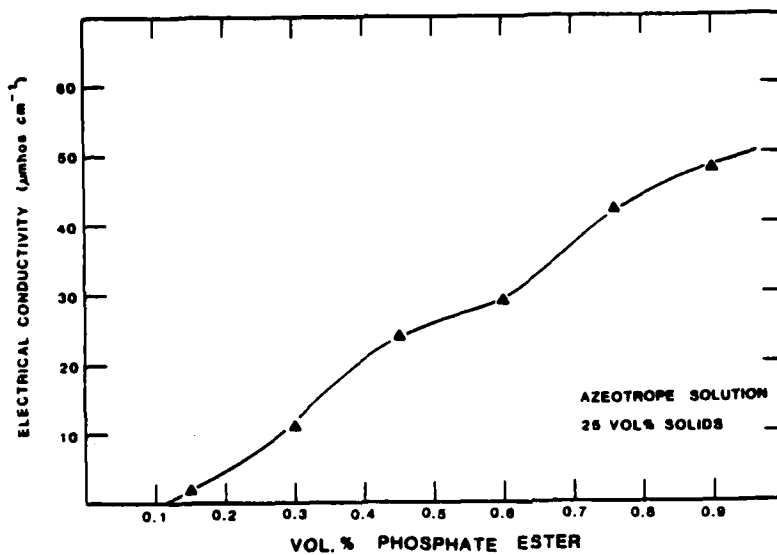


Figure 13 Conductivity as function of phosphate ester concentration.

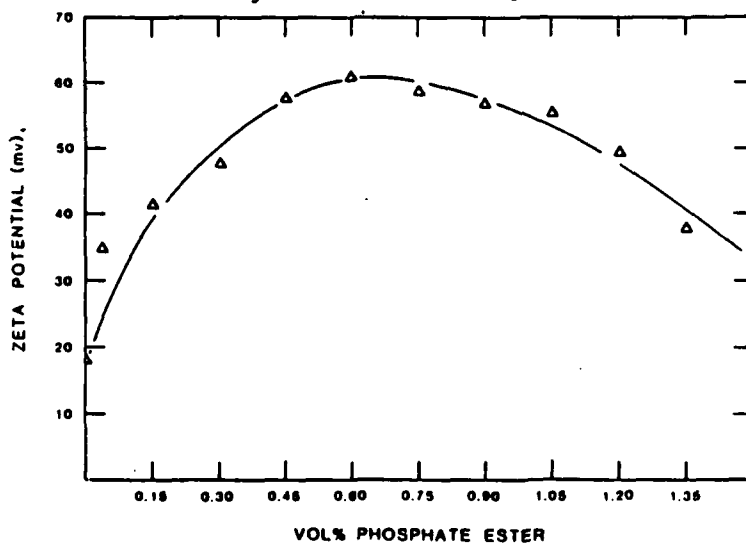


Figure 14 Zeta potential as a function of phosphate ester concentration

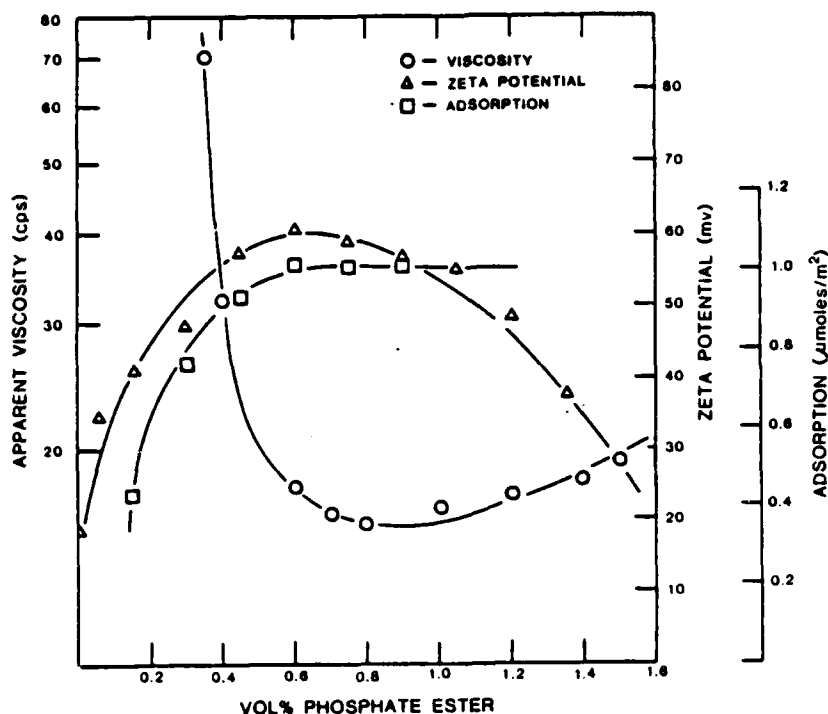


Figure 15 A comparison between zeta potential, viscosity and adsorption as a function of phosphate ester concentration.

II.1.2.7.2 Conductivity and Mobility as Function of Solvent Composition

Conductivity as a function of solvent fraction is shown in Figure 16 for supernatants of centrifuged suspensions. Conductivity increases and reaches a maximum on approach to the ethanol end member. The increase in conductivity was expected at high fractions of ethanol, since its dielectric constant (24.3) is higher than the MEK's (18.5). Thus, the ionic strength of the solution due to dissociation of the phosphate ester increased with increasing ethanol fractions. FTIR results may give us some insight into the reason for the maximum appearing in the curve near the MEK side of the binary. Results indicate that the carbonyl bond of the MEK is interacting with the hydrogen ion on the phosphate ester allowing it leave the phosphate ester as an ion. When the concentration of the MEK becomes very low the ionization is not as complete.

Figure 17 shows the zeta potential as a function of solvent composition. The data indicates a maximum zeta potential at the azeotrope solution of MEK/ethanol and a decrease in potential on either side of the azeotrope. A comparison of with the viscosity data, as shown in Figure 5, indicates a correlation between the maximum in the zeta potential and the optimum dispersion (i.e. minimum in viscosity). Both occurred at the azeotrope. Also, both the and degree of dispersion decrease on either side of the azeotrope solution. The decrease in viscosity at high ethanol fractions coincides with increased conductivity. It can be suggested that the increase in ionic strength at high ethanol fractions leads to a compression of the electrical double layer resulting in a decrease in , and thus, a decrease in dispersability.

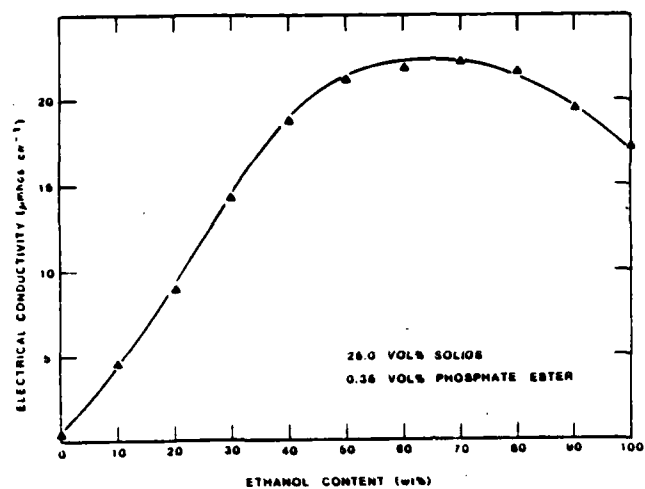


Figure 16 Conductivity as a function of solvent fraction.

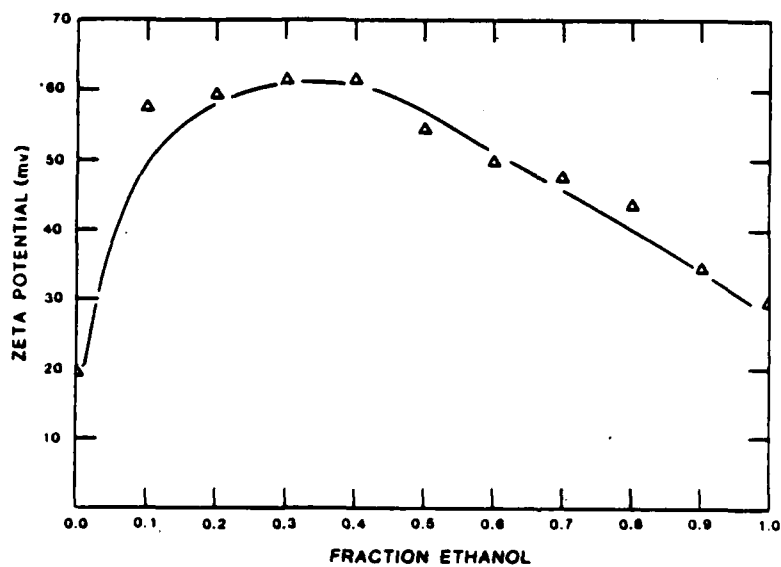


Figure 17. Zeta potential as a function of solvent fraction

II.1.3 Conclusions

The combination of electrostatic stabilization and steric stabilization is sometimes called electrosteric and both of these mechanisms may contribute to dispersion in our system; however, the dispersion data tends to follow the mobility data quite closely. This suggests the electrostatic mechanism may be the dominant mechanism and thus control stability. It should be noted that these mobility measurements were conducted on supernatants of centrifuged suspensions. The supernatant contained as dilute concentrations of particles originating from the concentrated suspension. Thus, mobility measurements were actually conducted on dilute suspensions. At very high solid concentrations, where interparticle distances approach a few A. At these distances the height of the energy barrier is smaller and electrostatic repulsion is less effective. The addition of a steric mechanism may prevent flocculation. Never-the-less, the trend in rheology of concentrated suspensions followed quite closely the trend in zeta potential suggesting that the electrostatic mechanism plays an important roll in stabilizing even the concentrated suspensions.

II.2 Interaction of Dispersant with the Binder and Other Organic Additives in the Slip. (John R. Morris, Jr.)

II.2.1 Introduction

Tape casting slips typically contain several components in addition to a dispersant: a binder, plasticizer/s, release agents, and possibly a homogenizer which prevents skin formation during drying. These components themselves may be good dispersants for the powder and when mixed with the dispersant may improve the dispersion of the powder. They may also react with the dispersant and cause increased flocculation. The organic components also react with the powder by adsorbing onto its surface. Thus the order of addition of the organics and the powder may effect the degree of dispersion of the powder. The object of this portion of the study is to determine the importance of these interactions.

Previous work (13) has shown that component addition sequence plays an important role in determining the viscosity of a tape casting slurry. However, the literature is confusing as to which technique produces superior tapes. Shanefield and Mistler (14) are advocates of premixing and milling the powder, solvent and dispersant before adding the other organic components. Some manufacturers of multilayer capacitors (15) find that good results are obtained by simply milling all the components together at one time. Still others find that adding the dispersant last gives the best results.

In this portion of our study, we have attempted to clear up some of the confusion regarding how the order of component addition affects the properties of the slurry, green tape, and sintered tapes. In order to determine these effects we have prepared slurries of identical composition using three component addition sequences, dispersant first, dispersant last, and simultaneous addition. The slurries were also aged for several days to determine if the effects of component addition sequence vary with slurry aging time.

The rheological properties of the slip, green density, and green tensile strength were measured and samples were sintered to determine sintered density, sintered strength, flatness, and electrical properties.

I.2.2 Experimental Procedures

II.2.2.1 Batch Preparation

The composition, consisting of commercially available barium titanate powder, a MEK-ethanol solvent system, an acrylic binder, two plasticizers (butyl-benzyl-phthalate, and polyethylene glycol 400), and a phosphate ester dispersant, was chosen as a model slurry. The acrylic binder, Acryloid B-7 MEK from Rohm and Haas was chosen due to wide commercial use and clean burnout. The plasticizers were selected on the basis of compatibility with the binder. The phosphate ester dispersant, Emphos PS-21A from Whitco Chemicals, was shown to be a very effective dispersant for this system in earlier work (1).

Three batches of identical composition were prepared as outlined in Figure 18, using three different component addition sequences: dispersant first; dispersant last; and simultaneous addition. In the dispersant first case, the solvent, dispersant, and powder were premixed, ultrasonically agitated for 2 minutes, and allowed to age for 24 hours before the remaining components were added. In the dispersant last case, all components except the dispersant were premixed, ultrasonically agitated, and aged for 24 hours before the dispersant was added. In the simultaneous addition slurry, all of the liquid components were premixed, ultrasonically agitated, and aged before addition of the powder. After the final components were added, all batches were again ultrasonically agitated for 2 minutes and the slurries were placed on a slow roller mill for the duration of the study. There were no grinding media added to the slurries as the purpose of the slow rolling action was to simply keep the components from separating during the aging study. The slurries were removed from the slow roller mill only for sample taking.

BATCH A (DISPERSANT FIRST)	BATCH B (DISPERSANT LAST)	BATCH C (SIMULTANEOUS ADDITION)
36% BARIUM TITANATE 33.5% MEK/ETHANOL 0.75% PHOSPHATE ESTER	36% BARIUM TITANATE 33.5% MEK/ETHANOL 20% ACRYLIC BINDER 5% PEG 400 5% BUTYL BENZYL PHTHLATE 1% CYCLOHEXANONE	33.5% MEK/ETHANOL 20% ACRYLIC BINDER 5% PEG 400 5% BUTYL BENZYL PHTHLATE 0.75% PHOSPHATE ESTER 1% CYCLOHEXANONE
SONICATE 2 MIN. AGE 24 HR.	SONICATE 2 MIN. AGE 24 HR.	SONICATE 2 MIN. AGE 24 HR.
ADD: 20% ACRYLIC BINDER 5% PEG 400 5% BUTYL BENZYL PHTHLATE 1% CYCLOHEXANONE	ADD: 0.75% PHOSPHATE ESTER	ADD: 36% BARIUM TITANATE

Figure 18. The processing and addition sequence used in preparation of samples.

At twenty-four hour intervals slurry viscosity was measured and tapes from each batch were cast onto glass. A Cladan laboratory scale caster was used. The tapes were stripped from the casting glass after a twenty-four hour drying period and samples of the appropriate shapes for property measurements were cut.

II.2.2.2 Property Measurement

Properties of the slurry, the green tape, and the sintered tape were measured in order to determine if component addition sequence plays a significant role in determining tape characteristics. Specifically, viscosity, green density, green tensile strength, sintered density, sintered thickness, sintered flatness, sintered strength, and electrical properties were evaluated.

Viscosity was measured using a Brookfield cone-plate viscometer (Model 2X-HAT) at shear rates ranging from 3.84 to 384 reciprocal seconds. In some cases the slurry was too viscous to be measured at the highest shear rates, so the value was extrapolated from data at lower shear rates. This was done by plotting shear stress versus shear rate as shown in Figure 19, extrapolating the least squares line through the data out to 384 reciprocal seconds and determining the corresponding shear stress. Multiplying this value by the appropriate viscometer constants gives the viscosity. Relative viscosity was determined by measuring the viscosity of the complete slurry and that of the fluid components using a Haake Bucher rotating cup viscometer at a shear rate of 9.8 sec^{-1} .

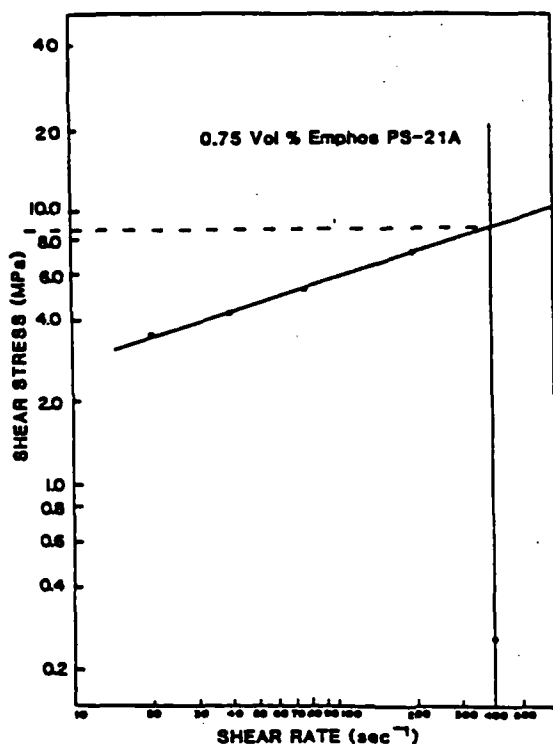


Figure 19. Method of extrapolation from low shear rates to high shear rates.

Green density was determined from geometrical measurements and sample weights. Weights were measured before and after binder burnout on a Mettler analytical balance accurate to 0.00001 grams. Volume was determined by cutting one inch square samples, and by measuring the thickness using a Mitutoyo thickness gage accurate to 0.0001 in. To eliminate variations in measured thickness due to deformation under the load of the measuring platens, the samples were placed between two pieces of precision machined glass (variation of less than 0.00005 in. in a square inch sample). This technique was found to give very consistent and reproducible data although some overestimation of volume with subsequent underestimation of density is inevitable.

Green tensile strength was measured by the technique described in reference 16. Briefly, this method involves cutting dog-bone shaped testing samples from the green tape using a scalpel, and testing them on an Instron universal testing machine. Air pressure actuated grips were used to minimize tearing which occurred when standard mechanical grips were used, and the loading rate was 2.5 cm/min, which corresponds to the plateau region of the stress strain curve.

The tapes were sintered using a heating schedule similar to that in Figure 20. Slow heating (1 degree C. per minute) to 500 degrees C. followed by a one hour hold was employed to facilitate complete burnout of all organics. Rapid heating to the firing temperature was followed by a one hour soak and cooling to room temperature. The ultimate firing temperature ranged from 1325 to 1375 degrees C.

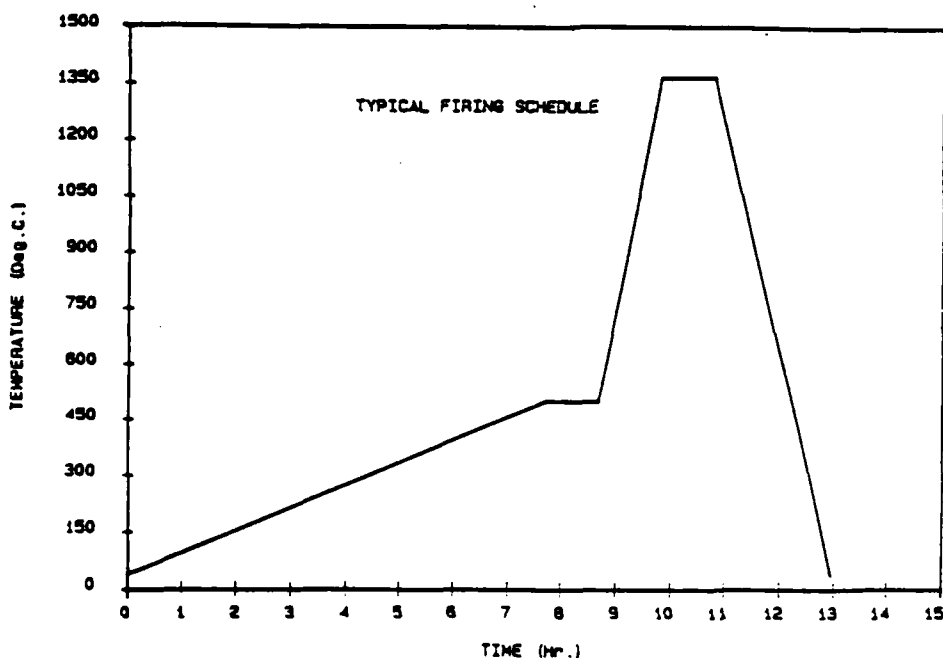


Figure 20. Heating schedule for sintering of tapes.

Fired density was measured by a geometrical technique similar to that used to evaluate the green tapes. In this instance, however, there was no need to place the samples between glass plates in order to measure the thickness since the sintered tapes did not deform under the load applied by the thickness gage. Geometrical measurement was found to give much more reproducible results than immersion techniques for measuring the density of these thin samples.

Fired strength was measured using a biaxial flexure technique described by Wachtman et al. (16). The fixture, shown in Figure 21, consists of an aluminum cup on the inside surface of which are machined three holes. Ball bearings are placed in the holes to act as sample supports. The disc shaped sample is placed on the bearings and a fourth ball bearing in which a flat surface has been machined is placed flat surface down in the center of the disc. The assembly is then placed on the load cell of an Instron universal testing machine and the load is applied to the upper ball.

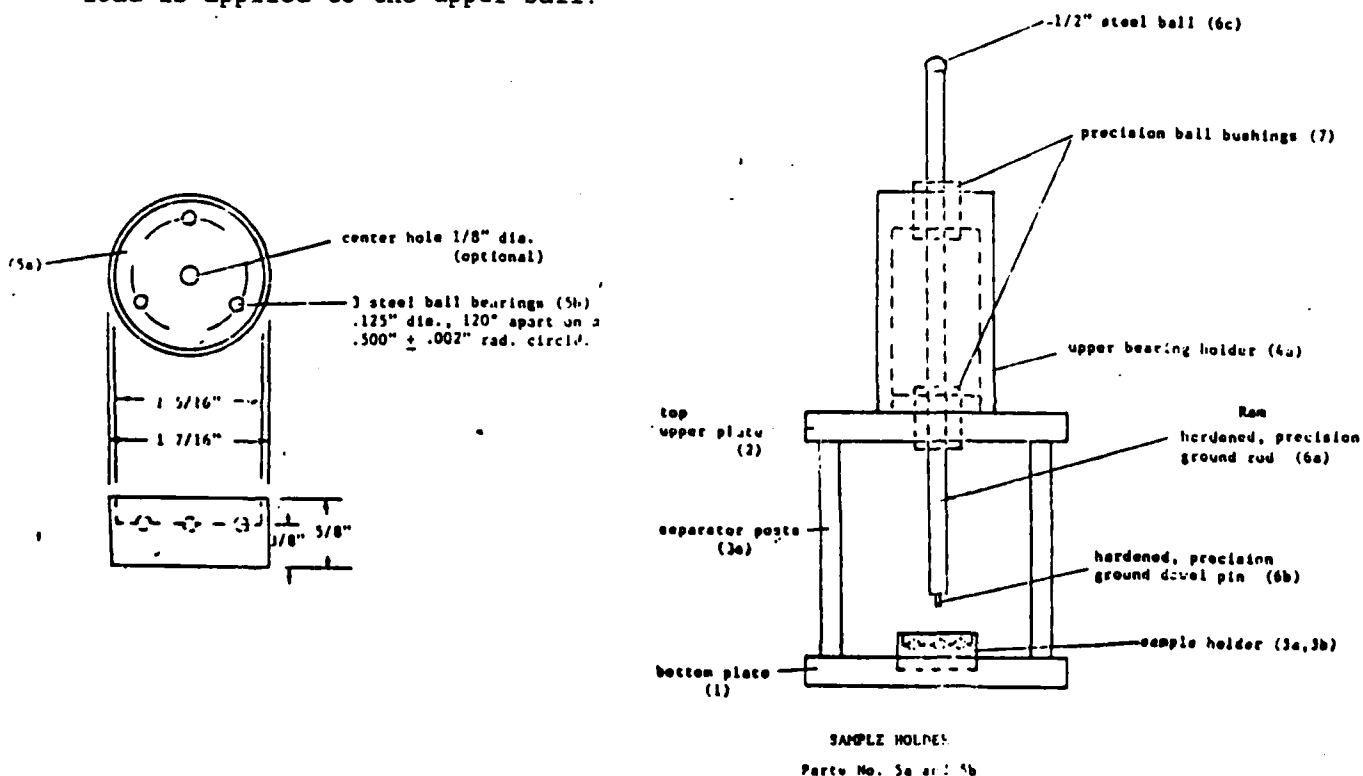


Figure 21. Schematic of fixture used for biaxial flexure tests.

Fired flatness was evaluated in a semi-quantitative way by observing the camber of the biaxial flexure discs before breaking them, and rating the flatness on the scale from one to four. As shown in Figure 22, four corresponds to no observed warpage and one corresponds to highly warped, ie. potato chip like. Twelve samples were averaged for each data point.





4.0	FLAT	
3.0	VERY SLIGHTLY WARPED	
2.0	SLIGHTLY WARPED	
1.0	WARPED	

Figure 22.- The scale for rating flatness.

Dielectric constant and dielectric loss were measured over a large range of frequencies. Difficulty was encountered in measuring the individual tapes due to their thickness (0.005 to 0.006 in.) so measurements were performed on thicker samples made of approximately twenty individual tape samples. These specimens were fabricated by laying up partially dried green tapes in a rectangular die and pressing them to bind the layers together. These multilayer structures were then sintered using the same schedule as the individual tapes, and cut into pieces suitable for measurement. This technique produces samples which more closely resemble actual multilayer capacitor structures than other thick samples such as slip cast or dry pressed bars.

II.2.3 Results and Discussion

II.2.3.1 Viscosity Measurements

Viscosity was measured over a range of shear rates in order to understand the rheological behavior of the system more completely than if single shear rate data were used. High shear rate measurements, which are of theoretical interest because at high shear rates flow is laminar and the behavior is newtonian⁸, were performed at or extrapolated to 384 sec^{-1} . These data are plotted in Figure 23. In the dispersant first case, viscosity is initially low, and with slurry aging time it increases to a constant value of approximately 300 centipoise. In the dispersant last case the trend is the opposite. On the

first day the viscosity is high, and with slurry aging time it decreases to a constant value of approximately 500 centipoise. In the simultaneous addition case, the viscosity remained virtually constant at 410 centipoise. The high shear rate viscosity data can possibly be explained in terms of competition for adsorption sites between the dispersant and another component (probably the binder). In the dispersant first case, the binder is strongly adsorbed to the surface of the powder, before the other components are added. The rapid, strong adsorption of the phosphate ester was demonstrated in an earlier study (1). This strongly adsorbed phosphate ester is a very effective dispersant, consequently, the viscosity is initially low in this case. With time, however, the binder (or possibly a plasticizer, or a combination of several components) replaces some of the phosphate ester on the powder surface, decreasing its effectiveness as a dispersant, thus increasing the viscosity of the slurry. In the dispersant last case, if we assume that the binder is initially strongly adsorbed on the surface of the powder, the behavior is the opposite of that in the dispersant first case. As the slurry is aged the phosphate ester replaces the binder on the powder surface, and the viscosity is lowered. It is interesting to note that while dispersant first slurry viscosity increases and dispersant last slurry viscosity decreases with slurry aging time the two curves do not converge to some equilibrium value (during the time frame of our study). This indicates that the affects of component addition sequence are part transient and part permanent (in a practical time scale).

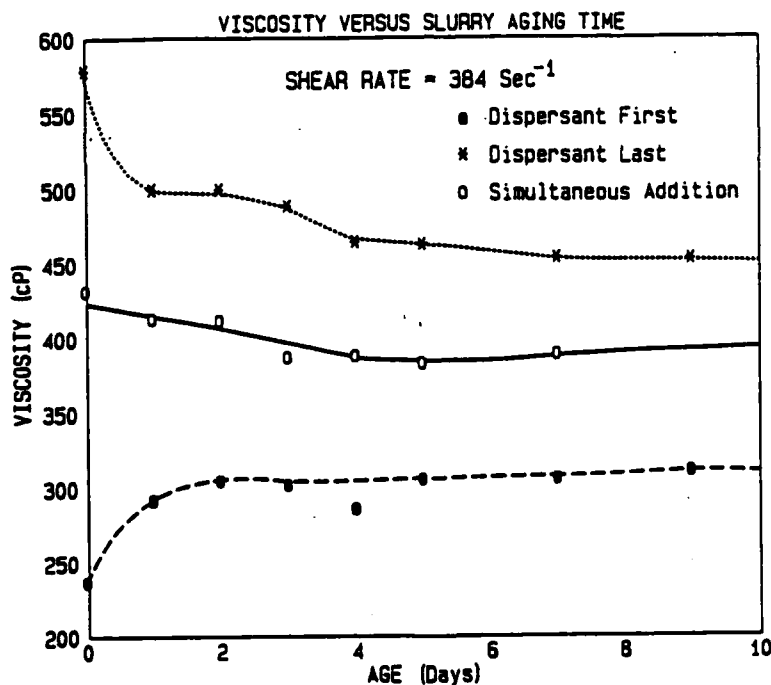


Figure 23. Viscosity measured at 384 sec⁻¹ as a function of aging time of the slip.

Viscosity was also plotted versus slurry aging time for all three component addition sequences when measured at 9.8 sec^{-1} . As can be seen in Figure 24, these results are very different from the high shear rate data. At this low shear rate the floc structure of the slurry and the strength of these flocs play important roles in determining the slurry viscosity. At the low shear rate, slurries made by simultaneous addition of the components have the highest viscosities, with the first day value being by far the largest. This can be interpreted to mean that these slurries have the greatest concentration of flocs or agglomerates, and that these are most prevalent in the first day of the aging study. Dispersant first and dispersant last slurries appear to have nearly the same viscosities throughout the aging study with a mean value of approximately 1200 centipoise.

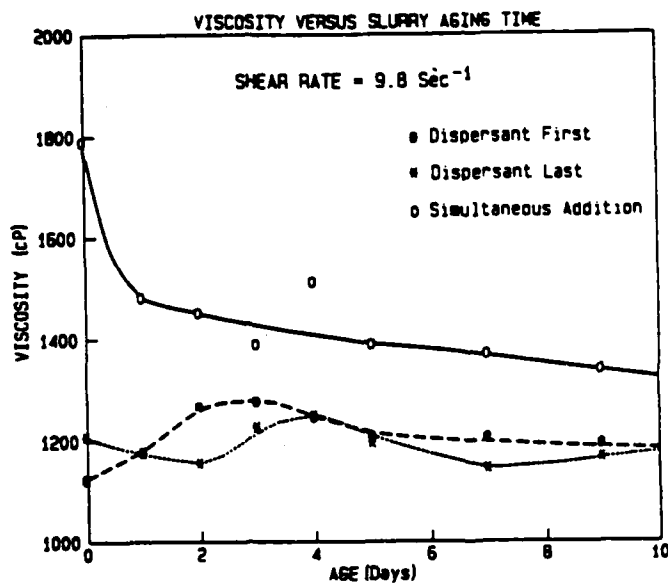


Figure 24. Viscosity measured at 9.8 sec^{-1} as a function of aging time of the slip.

In order that viscosity measurement have a practical application to tape casting they must be made at similar shear rates to that experienced by the slip during the casting process. There are a variety of shear rates experienced by the slip as it passes underneath the blade. A simple calculation of the average shear rate is

$$\dot{\gamma} = \frac{v}{d}$$

where d is the distance between the doctor blade and the substrate and v is the relative velocity between the blade and the substrate. This would yield for our system a value of about 500 sec^{-1} . Since however, our interest is determining the shear rate that best represents the state of agglomeration as the tape is layed down on the substrate, it may not be as a rapid shear rate at all. Rather it is likely that the very slow shear rate associated with the flow of the slip after it has passed the blade. Thus the data of Figure 24 (9.8 sec^{-1}) is of more practical interest. These results indicates that the degree of agglomeration in dispersant first and dispersant last slurries are similar and that they should behave similarly under casting conditions. The thickness measurements of the cast tapes shows the same trend, with dispersant first day one tapes being 0.005 in., dispersant last day one tapes measuring 0.005 in., and simultaneous addition day one tapes measuring 0.007 in thick.

II.2.3.2 Relative Viscosity

Relative Viscosity, which is defined as the viscosity of the suspension divided by that of the fluid components, can be used as a measure of component interaction. When a component of high intrinsic viscosity such as a binder is added to a slurry, it greatly increases the overall viscosity. However, as shown in our earlier study performed at a high shear rate (13), it can affect the relative viscosity quite differently, ie. the relative viscosity with the binder and other components was lower than the relative viscosity of the powder and solvent only. The current work extends these results to the low shear rate region of practical interest, and to three different component addition sequences. Components were added dispersant first, dispersant last, and binder, dispersant, plasticizer, plasticizer, homogenizer.

As can be seen in the tabular data in Table III, or in the bar graphs of Figures 25, 26, and 27, the suspension viscosity and relative viscosity vary greatly. When forming the initial slurries, the phosphate ester dispersant produces a much lower suspension viscosity than the acrylic binder, but the relative viscosities are similar. However, once the initial slurry is made, the effect of adding a particular component is consistent. Adding the binder or dispersant results in a marked decrease in relative viscosity. Incorporating the first plasticizer, butyl benzyl phthalate (Santicizer 160), always decreases the suspension viscosity and the relative viscosity. Conversely, addition of the second plasticizer, polyethylene glycol 400 (Carbowax 400), always increases the overall viscosity and the relative viscosity. Finally, the homogenizer cyclohexanone decreases both overall viscosity and relative viscosity.

Table III. The relative viscosity for slips with three different addition sequences.

COMPONENTS	VISCOSITY (Cp)		RELATIVE VISCOSITY
	FLUID COMPONENTS	TOTAL SUSPENSION	
SDP	0.64	314.9	492.0
SDP,B	27.0	4316.9	159.9
SDP,B,Sa	28.2	2956.8	104.8
SDP,B,Sa,C	31.5	4908.3	155.8
SDP,B,Sa,C,H	30.3	4387.4	144.8
SBP	28.2	14192.8	503.3
SBP,Sa	28.0	13897.2	496.3
SBP,Sa,C	33.0	17149.7	519.7
SBP,Sa,C,H	30.4	12714.4	418.2
SBP,Sa,C,H,D	30.0	5322.3	177.4
SBP	28.2	14192.8	503.3
SBP,D	28.8	6431.1	223.3
SBP,D,Sa	28.2	4730.9	167.7
SBP,D,Sa,C	33.6	5617.9	167.2
SBP,D,Sa,C,H	31.5	4583.0	145.5

KEY: S=solvent, D=dispersant, P=powder, Sa=Sanil60, C=Carbowax, H=homogenizer, B=binder

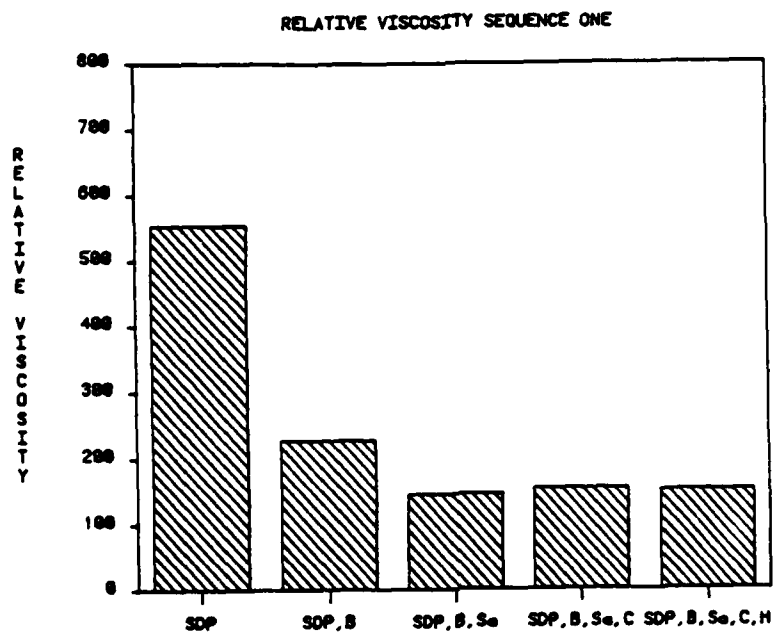


Figure 25. The relative viscosity measured for sequence 1.

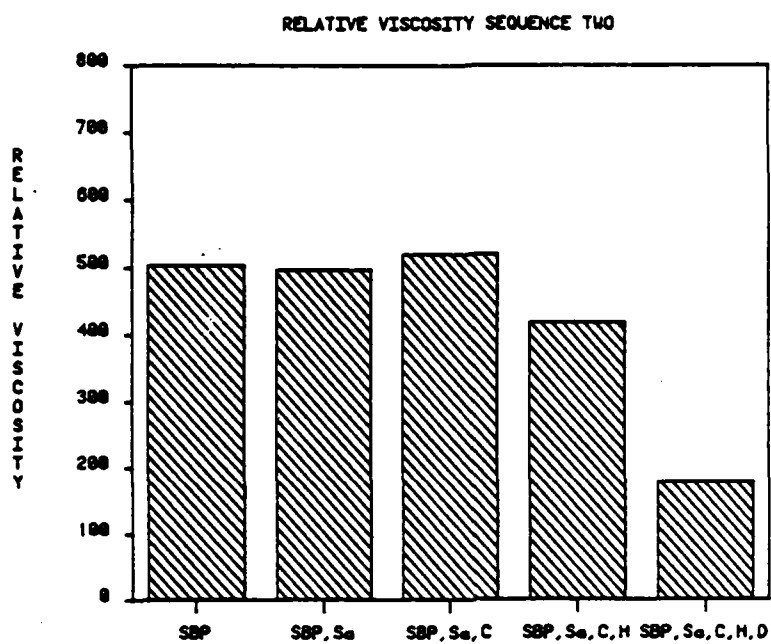


Figure 26. The relative viscosity measured for sequence 2.

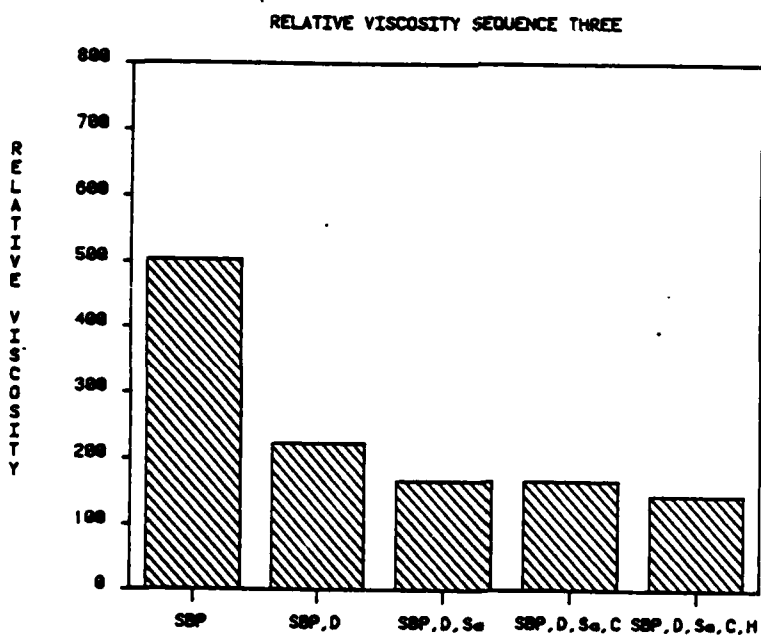


Figure 27. The relative viscosity measured for sequence 3.

In comparing these results to those of our earlier work, we see that the effect of adding a particular component to the slurry can be different depending on the shear rate. While adding dispersant, binder, or butyl benzyl phthalate always decreases relative viscosity polyethylene glycol 400 or cyclohexanone can either increase or decrease relative viscosity at different shear rates. Polyethylene glycol 400 increases relative viscosity at low shear rates while it decreases relative viscosity at high shear rates. At low shear rates PEG 400 could be acting to promote formation of weak flocs, but at higher shear rates these flocs could be broken up and PEG 400 could act as a lubricant. Cyclohexanone decreases relative viscosity at low shear rates and causes it to increase at high shear rates. At low shear rates it could be acting to solubilize clumps of undissolved binder which are broken up at high shear rates. On the other hand at high shear rates, it may increase the solubility of the dispersant in the liquid to the extent that its adsorption characteristics are altered, and viscosity is increased.

11.2.3.3 Green and Fired Density

Green and sintered densities were measured for day one tapes of all three component addition sequences. First day tapes were measured because the largest difference in measured properties is expected on the first day, and because the majority of commercial operations cast tapes without aging the slurry. As can be seen in Figure 11, dispersant first tapes have the highest densities, dispersant last tapes have intermediate values, and simultaneous addition tapes are the least dense. This trend holds true for both the green and the sintered state. These results agree with the low shear rate viscosity measurements, as the least viscous and presumably best dispersed system produces the tapes with the most efficient packing and the most viscous slurry produces the least dense tapes.

Table III

DAY ONE DENSITY COMPARISON					
ADDITION SEQUENCE	GREEN DENSITY		FIRED DENSITY		
	³ g/cm	% Th.	³ g/cm	% Th.	
DISPERSANT FIRST	2.873	52.0	5.132	93.3	
DISPERSANT LAST	2.764	50.2	5.076	92.2	
SIMULTANEOUS ADD	2.694	48.9	4.821	87.6	

Figure 28. Density of green and sintered tapes.

II.2.3.4 Green Tensile Strength

Green tensile strength was measured as a function of slurry aging time for the three component addition sequences. As can be seen in Figure 12, the simultaneous addition tapes show the lowest strengths in all cases. In fact these tapes were so fragile that strength measurement was not possible for the first three days of the study, the tapes broke under their own weight as they were placed in the testing fixture. Dispersant first and dispersant last tapes were both significantly stronger than the simultaneous addition tapes, with dispersant first tapes being slightly stronger than dispersant last tapes. It is believed that a chemical reaction occurs between the binder and one of the other components (probably the dispersant) which affects the ability of the binder to hold the powder particles together. Some preliminary infra-red data suggests that adding the phosphate ester to the acrylic binder affects the C-C and C-O bonding in the acrylic structure. Such a reaction could be used to explain the difference in strength between tapes made by the three different component addition sequences. In the simultaneous addition case, the fluid components of the slurry are allowed to premix for 24 hours in the absence of powder, giving this reaction the greatest opportunity to occur resulting in the weakest tapes. In the other two cases, the reaction occurs to a much lesser extent because the phosphate ester is adsorbed on the surface of the powder making it unavailable to react with the binder. The slight difference in strength between the dispersant first and dispersant last tapes can also be explained by similar reasoning. In the dispersant first case, the majority of the phosphate ester is adsorbed on the powder surface when the binder is added, while in the dispersant last case the phosphate ester can either adsorb on the powder or react with the binder. Hence, the reaction can more readily occur in the dispersant last case than in the dispersant first case, making the dispersant first tapes slightly stronger.

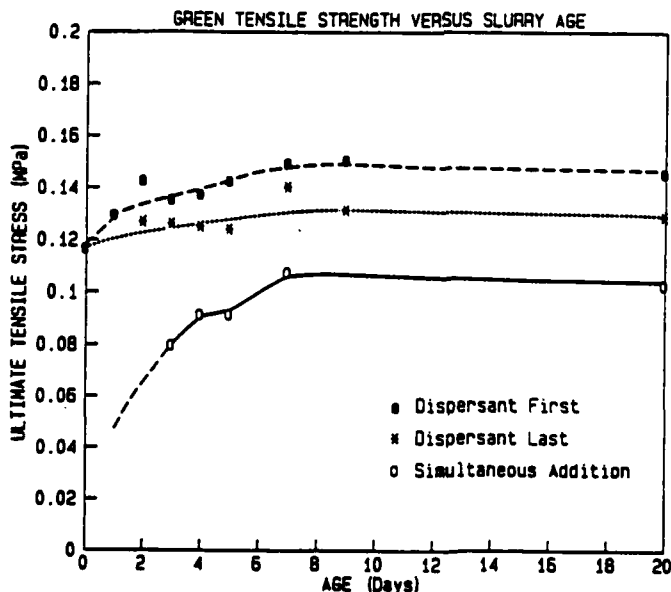


Figure 29. The ultimate tensile strength of green tapes.

In all cases, green tensile strength increased with slurry aging time. This could possibly be the result of a reversibility in the reaction proposed above or more probably due to a change in the microstructure of the tapes. Figures 13, 14, and 15 show SEM micrographs of the as cast surfaces of tapes made by all three component addition sequences, for Day 1, Day 6, and Day 10 of the aging study respectively. On the first day the microstructures of the dispersant first and dispersant last tapes appear to be fairly uniform with no gross flaws being visible. However, this is not the case for the simultaneous addition tapes, where pores, uncoated particles, and clumps of binder are clearly visible. These inhomogenieties are the most probable cause of the low strength of these tapes. After six days, the dispersant first and dispersant last tapes again appear to be uniform, with only a few small flaws. The simultaneous addition tape has areas of uniform well bonded tape but contains large voids which limit the strength. Finally, after ten days, the dispersant first and dispersant last tapes begin to show some evidence of agglomeration, while the simultaneous addition tapes appear to be more uniform than earlier in the study.

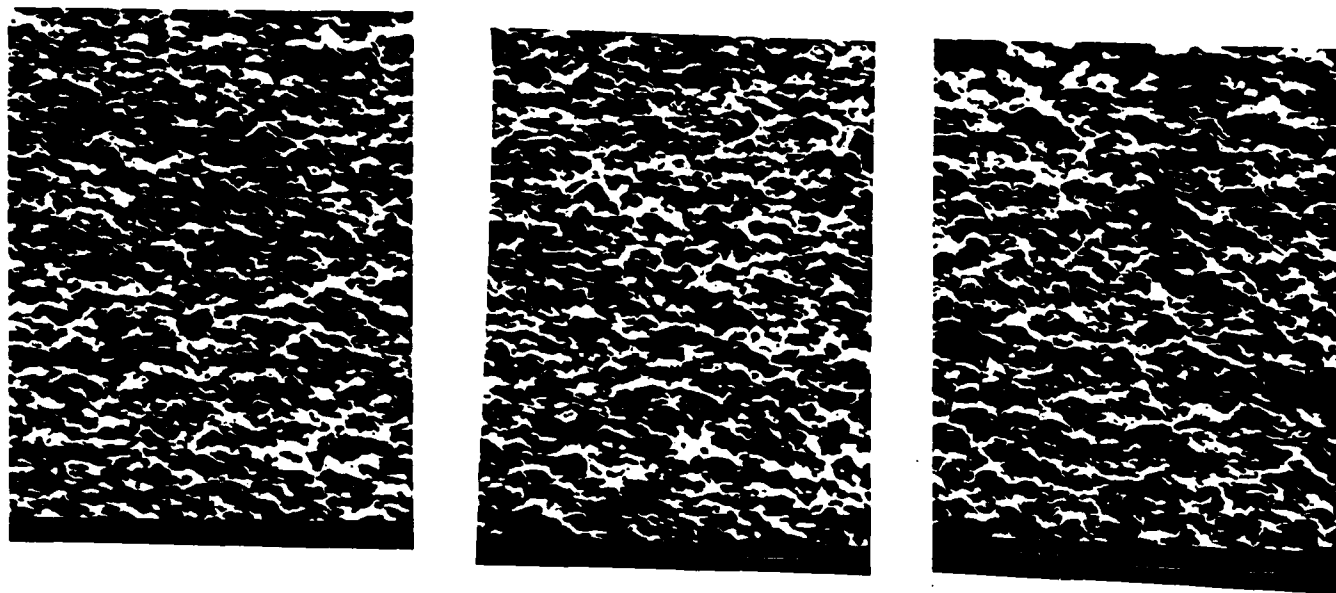
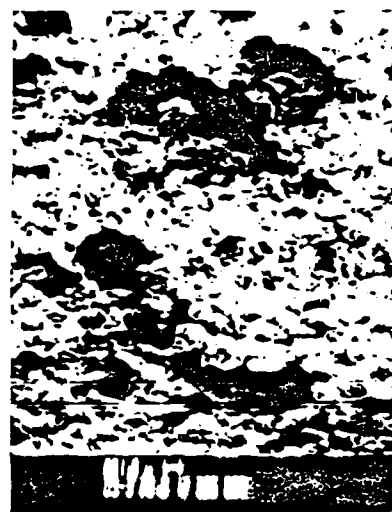
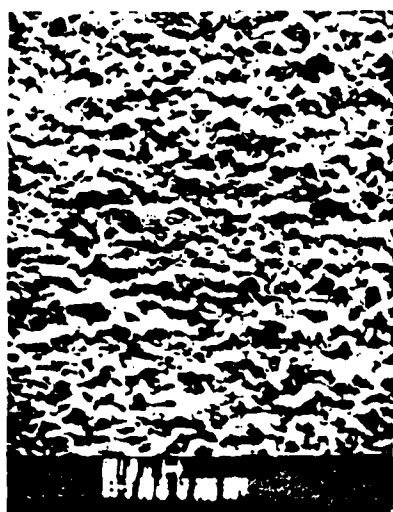
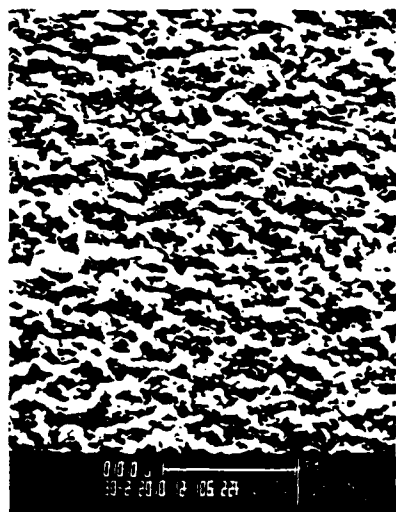
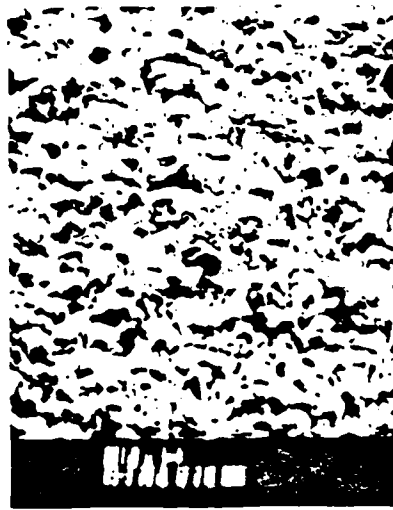
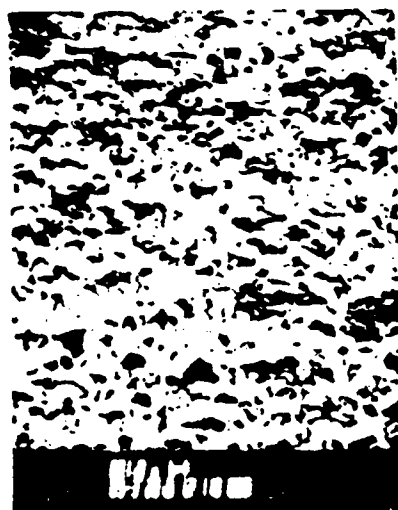


Figure 30. SEM micrograph of the as-cast surface of the various tapes for slips aged 1 day.



DISPERSANT FIRST DISPERSANT LAST SIMULTANEOUS ADDITION

Figure 31. SEM micrographs of the as-cast surface of the various tapes for slips aged 6 days.

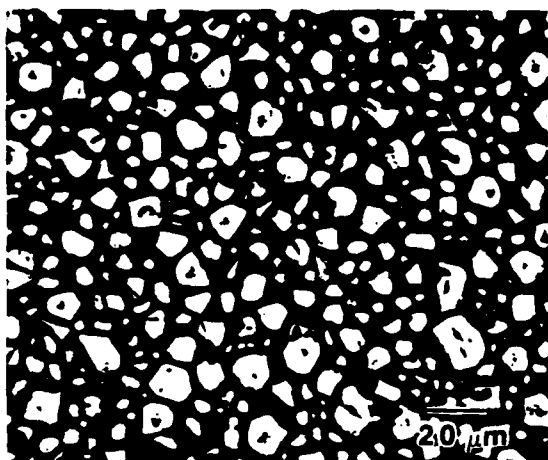


DISPERSANT FIRST DISPERSANT LAST SIMULTANEOUS ADDITION

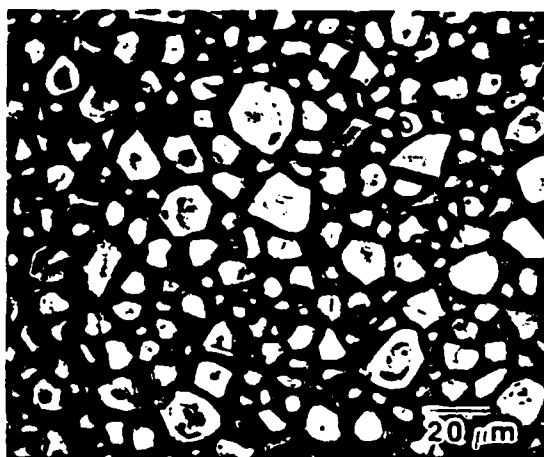
Figure 32. SEM micrographs of the as-cast surface of the various tapes for slips aged 10 days.

II.2.3.5 Sintering

The tapes were as described above for a one hour soak at temperatures ranging from 1325 to 1375 degrees C. The surfaces of the as-sintered tapes were then observed using optical microscopy, at a magnification of 400x. Optical microscopy was found to be a useful technique because of the relatively large size of the grains, and the large degree to which the grain boundaries are decorated by thermal etching. As can be seen in Figures 33, 34, and 35 this material exhibits a very short firing range. At 1325 °C. (Figure 33A) the material is undersintered and immature, and by 1375 °C. (Figure 35B) the microstructure is dominated by exaggerated grain growth. For the remainder of the study a firing temperature of 1365 °C. was chosen as a temperature at which the microstructure appears to be mature, but exaggerated grain growth is not observed.

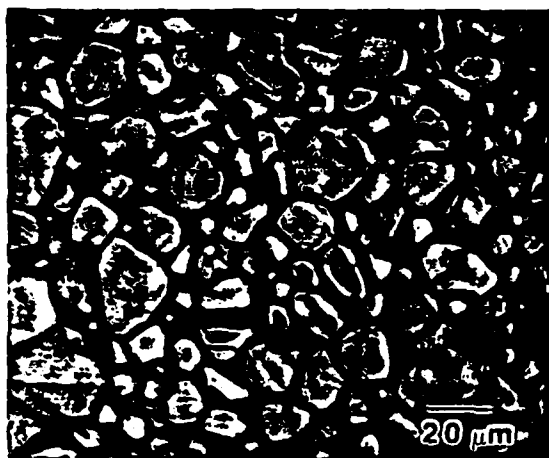


A. 1350°C



B. 1355 °C

Figure 33. Micrograph of as-sintered surface.



A. 1360 °C



B. 1365 °C

Figure 34. Micrograph of as-sintered surface.



A. 1370 °C



B. 1375 °C

Figure 35. Micrograph of as-sinter surface.

E. Fired Flatness

Fired flatness data for all three component addition sequences is plotted in Figure 36. In all cases the dispersant first tapes are the flattest, dispersant last tapes have intermediate values, and simultaneous addition tapes are the least flat. These results follow directly from the low shear rate viscosity data, and the density measurements. That is, tapes made from low viscosity slurries have more uniform packing, as evidenced by higher green density, and consequently less warpage during firing is observed.

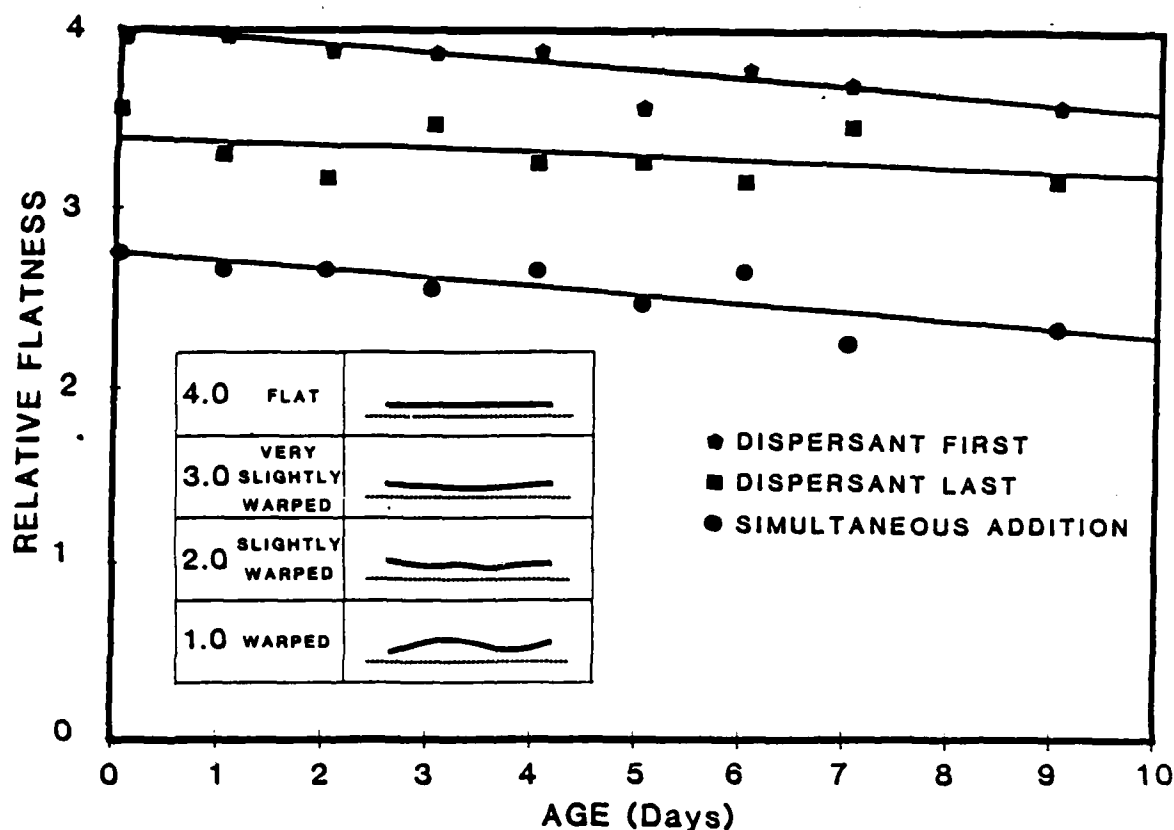


Figure 36. Flatness as a function of addition sequence and slip aging.

Another trend which can be seen in Figure 36, is a decrease in flatness with slurry aging time for tapes made by all component addition sequences. This behavior is not easily explained in terms of any of the other measurements made in this study, and is simply presented as an empirical observation.

II.2.3.6 Sinter Tape Strength

The strength of sintered tapes, as measured by biaxial flexure, is plotted in Figure 37. There appears to be very little difference between the three component addition sequences after the second day of the aging study, but there appears to be a significant difference in the first day. The simultaneous addition tapes are much weaker than either dispersant first or dispersant last tapes in this case. This is an important result because on the first day the affects of adding the components in different sequences should be most pronounced, and because most commercial tapes are made from unaged slurries. The low strength of the day one simultaneous addition tapes can be traced to large (100 to 200 micron) flaws which have be observed only in these tapes. Figure 38 shows these flaws in a SEM micrograph of the as sintered surface. These flaws are probably the result of agglomerates in the slurry which cause poor packing in the green state, and differential sintering.

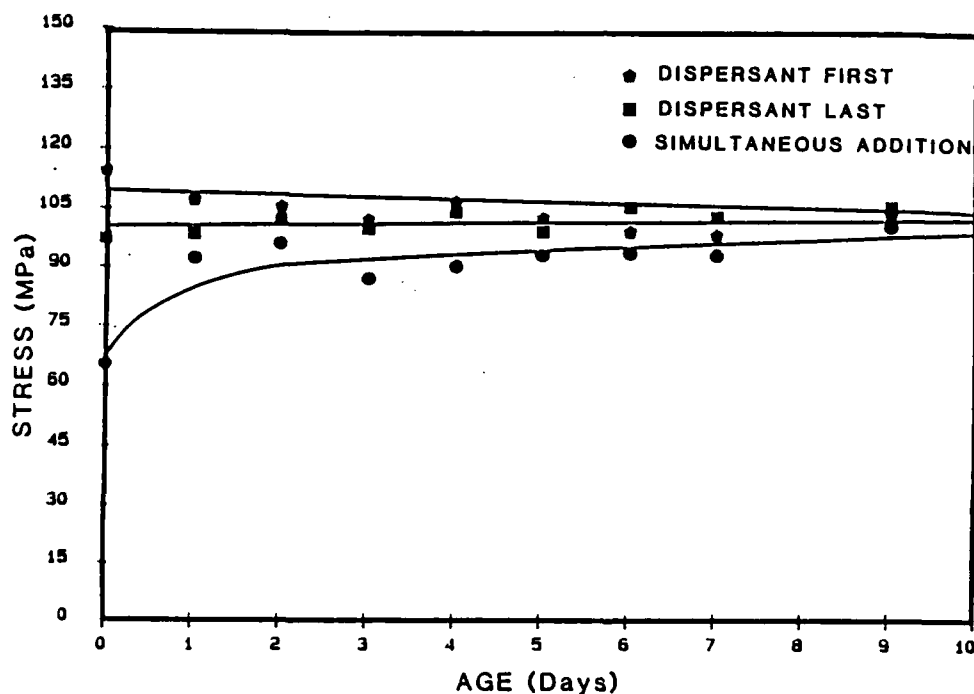


Figure 37. The biaxial flexure strength of sintered tapes as a function of addition sequence and aging time.

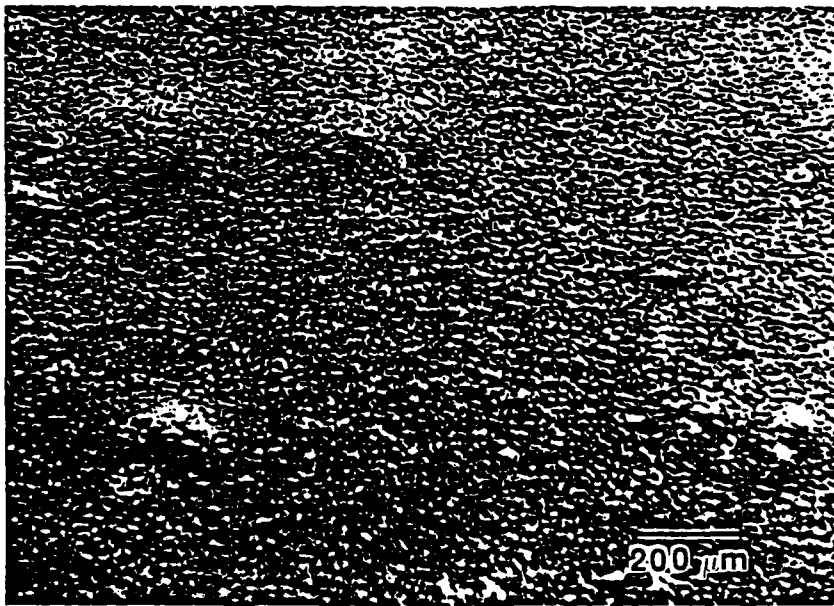


Figure 38. The surface of a sintered tape made from slips using the simultaneous addition sequence.

II.2.3.7 Electrical Properties

Dielectric constant and dielectric loss were measured over a large range of frequencies (1 khz to 10 Mhz). The early results indicated that dielectric constant varied with thickness. For tapes with thicknesses of 0.125 mm to 0.150 mm the dielectric constant is approximately 800 whereas thicker tapes made by multilaying the thinner tapes had a dielectric constant of 1600. The values for the thinner tapes as well as their standard deviations is shown in Table IV. Differences in the dielectric constants arise from their thickness differences but the standard deviation we feel depends on the addition sequence. On the few measurements made on the thicker samples this trend of higher standard deviation is reinforced. The standard deviation is higher when for the simultaneous addition sequence.

TABLE IV. The dielectric constant of tapes made with the three addition sequences.

II.2.4 Conclusions

In section II.1 it was concluded that the phosphate ester-barium titanate dispersion mechanism was primarily an electrostatic-static one. In this section two results were observed. First, it was observed that the relative viscosity of the slips decreases with addition of the binder (other components have less effect or even increase relative viscosity). Second, it was observed that the addition sequence has considerable effect on the state of dispersion and the subsequent properties of the slip and the green and sintered tape. It has been stated in the text that the degree of dispersion depends on which component adsorbs onto the surface of the powder first. This explanation, however, is incomplete. The phosphate ester produces a electrostatic repulsion and the binder, likely, a steric repulsion. The phosphate ester need not adsorb on the surface to accomplish the electrostatic repulsion. During the coming year this topic will be considered more fully.

REFERENCES

1. W.R. Cannon. "Deflocculants for Tape Casting Barium Titanate", Tech. Report No. 3; July, 1984; contract No. N0014-82-K-0313; Prepared for the Office of Naval Research, 800 N. Quincy St., Arlington, Virginia 22217; Rutgers, The State University of N.J., Piscataway, N.J.
2. W.R. Cannon, "O Deflocculants for Tape Casting Barium Titanate Dielectrics; March, 1983, Contract No. N0014-82-K-0310, Prepared for the ONR; Rutgers, The State University, Piscataway, N.J.
3. F.M. Fowkes, "Mechanisms of Electric Charging Particles in Nonaqueous Liquids," Reprinted from ASC Symposium Series, No. 200, 1982.
4. T. Sato and R. Ruch, Stabilization of Colloidal Dispersions by Polymer Adsorption, Marcel Dekker, Inc., N.Y., 1980.
5. D.J. Shaw, Introduction to Colloid and Surface Chemistry, 3rd ed., Butterworth and Co. Ltd., 1980.
6. M. Heathe, Whitco Chemical Co., New York, N.Y., private conversation, January 1983.
7. A.M. James "Electrophoresis of Particles in Suspension", in Surface and Colloid Science Vol. 2 Ed. R.J. Good and R.R. Stromberg Plenum, Press, N.Y.
8. Henry, D.C., Proc. Roy. Soc., A133 (1931) 106.
9. Wiersema, P.H. Loeb, A.L., and Overbeek, J. Th., J. Colloid Interface Sci., 22 (1966) 78-99.
10. O'brien, W.O. and White, L.R., J. Chem. Soc., Faraday Trans II, 74 (1978) 1607-1629.
11. J.J. Kipling, Adsorption from Solution of Non-Electrolytes, Academic Press, Inc., N.Y., 1965.
12. A. Klinkenburg and J. L. Landau, "Electrostatics in the Petroleum Industry", Elsevier, 1958, p. 40.
13. L. Braun, J. R. Morris, Jr., W. R. Cannon, "Viscosity of Tape-Casting Slips", Am. Ceram. Soc. Bull. 64, (5), May, 1985, pp. 727-729.
14. S. Forti, J. R. Morris, Jr., W. R. Cannon, "Strength of Cast Tapes", Am. Ceram. Soc. Bull. 64, (5), May, 1985, pp. 724,725
15. D. J. Shanefield, R. B. Runk, R. E. Mistler, in Ceramic Processing Before Firing, Ed. by G. Onoda, L. Hench, Wiley and Sons, NY, 1978.
16. D. W. Hamer, Viclan Ceramic Capacitor Handbook, Viclan, Inc., San

Diego, CA

17. K. R. Mikeska, M. S. Thesis, Rutgers University, 1984.
18. J. B. Wachtman, et. al., "Biaxial Flexure Tests of Ceramic Substrates", J. Materials, 7, (2), 1972, pp. 188-194.
19. G. W. Phelps, Rheology and Rheometry of Clay-Water Systems, Cypress Press, 1980.
20. R. J. MacKinnon, M. S. Thesis, Rutgers University, 1983.



DEPARTMENT OF THE NAVY

OFFICE OF NAVAL RESEARCH

ARLINGTON, VIRGINIA 22217

IN REPLY REFER TO

BASIC DISTRIBUTION LIST

Technical and Summary Reports

December 1982

<u>Organization</u>	<u>Codes</u>	<u>Organization</u>	<u>Copies</u>
Defense Documentation Center Cameron Station Alexandria, VA 22314	12	Naval Air Propulsion Test Center Trenton, NJ 08628 ATTN: Library	1
Office of Naval Research Department of the Navy 800 N. Quincy Street Arlington, VA 22217 Attn: Code 431	3	Naval Construction Battalion Civil Engineering Laboratory Port Hueneme, CA 93043 ATTN: Materials Division	1
Naval Research Laboratory Washington, DC 20375 ATTN: Codes 6000 6300 2627	1 1 1	Naval Electronics Laboratory San Diego, CA 92152 ATTN: Electron Materials Sciences Division	1
Naval Air Development Center Code 606 Warminster, PA 18974 ATTN: Dr. J. DeLuccia	1	Naval Missile Center Materials Consultant Code 3312-1 Point Mugu, CA 92041	1
Commanding Officer Naval Surface Weapons Center White Oak Laboratory Silver Spring, MD 20910 ATTN: Library	1	Commander David W. Taylor Naval Ship Research and Development Center Bethesda, MD 20084	1
Naval Oceans Systems Center San Diego, CA 92132 ATTN: Library	1	Naval Underwater System Center Newport, RI 02840 ATTN: Library	1
Naval Postgraduate School Monterey, CA 93940 ATTN: Mechanical Engineering Department	1	Naval Weapons Center China Lake, CA 93555 ATTN: Library	1
Naval Air Systems Command Washington, DC 20360 ATTN: Code 31A Code 5304B	1 1	NASA Lewis Research Center 21000 Brookpark Road Cleveland, OH 44135 ATTN: Library	1
Naval Sea System Command Washington, DC 20362 ATTN: Code 05R	1	National Bureau of Standards Washington, DC 20234 ATTN: Metals Science and Standards Division Ceramics Glass and Solid State Science Division Fracture and Deformation Div.	1 1 1 1

::
RE/431/82/174

Naval Facilities Engineering
Command
Alexandria, VA 22331
ATTN: Code 03

1

Defense Metals and Ceramics
Information Center
Battelle Memorial Institute
505 King Avenue
Columbus, OH 43201

1

Scientific Advisor
Commandant of the Marine Corps
Washington, DC 20380
ATTN: Code AX

1

Metals and Ceramics Division
Oak Ridge National Laboratory
P.O. Box X
Oak Ridge, TN 37380

1

Army Research Office
P. O. Box 12211
Triangle Park, NC 27709
ATTN: Metallurgy & Ceramics
Program

1

Los Alamos Scientific Laboratory
P.O. Box 1663
Los Alamos, NM 87544
ATTN: Report Librarian

1

Army Materials and Mechanics
Research Center
Watertown, MA 02172
ATTN: Research Programs
Office

Argonne National Laboratory
Metallurgy Division
P.O. Box 229
Lemont, IL 60439

1

Air Force Office of Scientific
Research/NE
Building 410
Bolling Air Force Base
Washington, DC 20332
ATTN: Electronics & Materials
Science Directorate

1

Brookhaven National Laboratory
Technical Information Division
Upton, Long Island
New York 11973
ATTN: Research Library

1

Library
Building 50, Room 134
Lawrence Radiation Laboratory
Berkeley, CA

1

NASA Headquarters
Washington, DC 20546
ATTN: Code RRM

1

General Electric Company
P.O. Box 7722
Philadelphia, PA 19101

::
RE/431/84/46

January 1984

NEW MULTILAYER CAPACITOR PROGRAM LIST

Professor Harlan U. Anderson
University of Missouri-Rolla
107 Fulton Hall
Rolla, MO 65401

Professor R. Vest
Purdue University
West Lafayette, IN 47907

Dr. John B. Blum
Rutgers University
College of Engineering
P.O. Box 909
Piscataway, NJ 08859

Dr. J. V. Biggers
Pennsylvania State University
Materials Research Laboratory
University Park, PA 16802

Professor R. Buchanan
University of Illinois
Department of Ceramic Engineering
Urbana, IL 61801

Professor Larry Burton
Virginia Polytechnic Institute
and State University
Blacksburg, VA 24061

Professor Roger Cannon
Rutgers University
College of Engineering
P.O. Box 909
Piscataway, NJ 08859

Prof. Donald M. Smyth
Lehigh University
Materials Research Laboratory
Coxe Laboratory 32
Bethlehem, PA 18015

Dr. N. Eror
Oregon Graduate Center
19600 N. W. Walker Road
Beaverton, OR 97006

Dr. K. D. McHenry
Honeywell Ceramics Center
5121 Winnetka ave., N.
New Hope, MN 55428

Professor D. W. Readey
Department of Ceramic Engineering
1314 Kinnear Road
Columbus, OH 43212

Dr. Lew Hoffman
Hoffman Associates
301 Broadway (US 1) Suite 206A
P.O. 10492
Riviera Beach, FL 33404

Dr. Gordon R. Love
Corporate Research, Development
and Engineering
Sprague Electric Co.
North Adams, Mass 01247

Roger T. Dirstine
Ceramics Research
Unitrode Corporation
580 Pleasant St.
Watertown, Mass 02172

Dr. Sidney J. Stein
Electro-Science Laboratories
2211 Sherman Ave
Pennsauken, NJ 08110

John C. Constantine
Electronic Materials Systems
Englehard Industries Division
1 West Central Ave.
E. Newark, NJ 07029

::
RE/431/84/46

(Continue of Multilayer Capacitor Program List)

John Piper
Union Carbide Corporation
Electronics Division-Components Dept.
P.O. Box 5928
Greenville, SC 29606

Dr. Kim Ritchie
Vice President
Corporate Research Laboratory
AVX Corporation
P.O. Box 867
Myrtle Beach, SC 29577

Tack J. Whang
Technical Center
Ferro Corporation
7500 E. Pleasant Valley Road
Independence, OH 44131

Advanced Research Projects
Materials Science Director
1400 Wilson Boulevard
Arlington, VA 22209

Dr. Gene Haertling
Motorola Corporation
3434 Vassar, NE
Albuquerque, NM 87107

W.B. Harrison
Honeywell Ceramics Center
5121 Winnetka Ave. N.
New Hope, MN 55428

Prof. L. E. Cross
The Pennsylvania State University
Materials Research Laboratory
University Park, PA 16802

Dr. P.L. Smith
Naval Research Laboratory
Code 6361
Washington, DC 20375

Professor R. Roy
The Pennsylvania State University
Materials Research Laboratory
University Park, PA 16802

Dr. R. Rice
Naval Research Laboratory
Code 6360
Washington, DC 20375

Dr. G. Ewell
MS6-D163
Hughes Aircraft Company
Centinela & Teale Streets
Culver City, CA 90230

Dr. George W. Taylor
Princeton Resources, Inc.
P.O. Box 211
Princeton, NJ 08540

Dr. J. Smith
GTE Sylvania
100 Endicott Street
Danvers, MA 01923

Professor R. Buchanan
Department of Ceramic Engineering
University of Illinois
Urbana, Ill 61801

Dr. Wallace A. Smith
North American Philips Laboratories
345 Scarborough Road
Briarcliff Manor, NY 10510

Professor B. A. Auld
Stanford University
W.W. Hansen Laboratories of Physics
Stanford, CA 94306

Mr. G. Goodman, Manager
Corporation of Applied Research
Group
Globe-Union Inc.
5757 North Green Bay Avenue
Milwaukee, WI 53201

Director
Applied Research Lab
The Pennsylvania State Univ.
University Park, PA 16802

Additional Copies

Dr. Von Richards
Argonne National Lab
Materials Sci. Techn. Div.
Bldg. 212
9700 So. Cass Ave.
Argonne, ILL 60439

Dr. T. C. Dean
TAM Ceramics, Inc.
Box C
Bridge Station
Niagara Falls, NY 14305

Mr. Paul Baker
Bourns Inc.
693 West 1700 So. Street
Logan, UTAH 84321

Dr. David Cronin
Trans-Tech
S520 Adamstown Rd.
Adamstown, MD 21710

END
FILMED

5-86

DTIC